ORNL/TM-11181

ornl

OAK RIDGE
NATIONAL
LABORATORY

MARTIN MARIETTA

Comparison of Calculated Results with Experimental Data for the Tritium Production Rates in a Li_2O Assembly

R. T. Santoro
R. G. Alsmiller, Jr.
J. M. Barnes
T. A. Gabriel

OAK RIDGE NATIONAL LABORATORY
CENTRAL RESEARCH LIBRARY
CIRCULATION SECTION
4500N ROOM 175
LIBRARY LOAN COPY
DO NOT TRANSFER TO ANOTHER PERSON
If you wish someone else to see this report, send in name with report and the library will arrange a loan.

OPERATED BY
MARTIN MARIETTA ENERGY SYSTEMS, INC.
FOR THE UNITED STATES
DEPARTMENT OF ENERGY

This report has been reproduced directly from the best available copy.

Available to DOE and DOE contractors from the Office of Scientific and Technical Information, P.O. Box 62, Oak Ridge, TN 37831; prices available from (615) 576-8401, FTS 626-8401.

Available to the public from the National Technical Information Service, U.S. Department of Commerce, 5285 Port Royal Rd., Springfield, VA 22161.
NTIS price codes—Printed Copy: A03 Microfiche A01

This report was prepared as an account of work sponsored by an agency of the United States Government. Neither the United States Government nor any agency thereof, nor any of their employees, makes any warranty, express or implied, or assumes any legal liability or responsibility for the accuracy, completeness, or usefulness of any information, apparatus, product, or process disclosed, or represents that its use would not infringe privately owned rights. Reference herein to any specific commercial product, process, or service by trade name, trademark, manufacturer, or otherwise, does not necessarily constitute or imply its endorsement, recommendation, or favoring by the United States Government or any agency thereof. The views and opinions of authors expressed herein do not necessarily state or reflect those of the United States Government or any agency thereof.

ORNL/TM-11181

Engineering Physics and Mathematics

Comparison of Calculated Results with Experimental Data for the Tritium Production Rates in a Li_2O Assembly

R. T. Santoro, R. G. Alsmiller, Jr.,
J. M. Barnes, and T. A. Gabriel

DATE PUBLISHED — May 1989

Submitted for Journal Publication

Prepared by the
OAK RIDGE NATIONAL LABORATORY
Oak Ridge, Tennessee 37831
operated by
MARTIN MARIETTA ENERGY SYSTEMS, INC.
for the
U.S. DEPARTMENT OF ENERGY
under contract DE-AC05-84OR21400

MARTIN MARIETTA ENERGY SYSTEMS LIBRARIES

3 4456 0299608 8

CONTENTS

ABSTRACT ix
1. INTRODUCTION 1
2. DETAILS OF THE CALCULATIONS 2
3. DISCUSSION OF RESULTS 7
REFERENCES 32

LIST OF FIGURES

Figure		Page
1	Plan View of the Experiment Room	10
2	Schematic of the Neutron Biasing Scheme	11
3	^{6}Li Tritium Production vs Distance in the Li_2O Assembly–Reference Case	12
4	^{6}Li Tritium Production vs Distance in the Li_2O Assembly with 0.5 cm–thick SS–304	13
5	^{6}Li Tritium Production vs Distance in the Li_2O Assembly with 1.5 cm–thick SS–304	14
6	^{6}Li Tritium Production vs Distance in the Li_2O Assembly with 0.5 cm–thick SS–304 and 0.5 cm–thick Polyethylene	15
7	^{6}Li Tritium Production vs Distance in the Li_2O Assembly with 1.5 cm–thick SS–304 and 0.5 cm–thick Polyethylene	16
8	Calculated–to–Experimental Ratio for ^{6}Li Tritium Production vs Distance in the Li_2O Assembly–Reference Case	17
9	Calculated–to–Experimental Ratio for ^{6}Li Tritium Production vs Distance in the Li_2O Assembly with 0.5 cm–thick SS–304	18
10	Calculated–to–Experimental Ratio for ^{6}Li Tritium Production vs Distance in the Li_2O Assembly with 1.5 cm–thick SS–304	19
11	Calculated–to–Experimental Ratio for ^{6}Li Tritium Production vs Distance in the Li_2O Assembly with 0.5 cm–thick SS–304 and 0.5 cm–thick Polyethylene	20
12	Calculated–to–Experimental Ratio for ^{6}Li Tritium Production vs Distance in the Li_2O Assembly with 1.5 cm–thick SS–304 and 0.5 cm–thick Polyethylene	21
13	^{7}Li Tritium Production vs Distance in the Li_2O Assembly–Reference Case	22

Figure		Page
14	^{7}Li Tritium Production vs Distance in the Li_2O Assembly with 0.5 cm–thick SS–304	23
15	^{7}Li Tritium Production vs Distance in the Li_2O Assembly with 1.5 cm–thick SS–304	24
16	^{7}Li Tritium Production vs Distance in the Li_2O Assembly with 0.5 cm–thick SS–304 and 0.5 cm–thick Polyethylene	25
17	^{7}Li Tritium Production vs Distance in the Li_2O Assembly with 1.5 cm–thick SS–304 and 0.5 cm–thick Polyethylene	26
18	Calculated–to–Experimental Ratio for ^{6}Li Tritium Production vs Distance in the Li_2O Assembly–Reference Case	27
19	Calculated–to–Experimental Ratio for ^{6}Li Tritium Production vs Distance in the Li_2O Assembly with 0.5 cm–thick SS–304	28
20	Calculated–to–Experimental Ratio for ^{6}Li Tritium Production vs Distance in the Li_2O Assembly with 1.5 cm–thick SS–304	29
21	Calculated–to–Experimental Ratio for ^{6}Li Tritium Production vs Distance in the Li_2O Assembly with 0.5 cm–thick SS–304 and 0.5 cm–thick Polyethylene	30
22	Calculated–to–Experimental Ratio for ^{6}Li Tritium Production vs Distance in the Li_2O Assembly with 1.5 cm–thick SS–304 and 0.5 cm–thick Polyethylene	31

LIST OF TABLES

Table		Page
1	Detector Locations and Monte Carlo Estimator Cell Dimensions .	4
2	53–Neutron Energy Group Structure and Tritium Breeding Cross Sections	5
3	Composition of Materials Used in the Calculation	6
4	Experimental Configurations Used for the Tritium Production Measurements	7

ABSTRACT

The Monte Carlo codes MORSE and MCNP have been used to calculate the tritium production from ≈14 MeV neutron reactions in a Li_2O assembly. Tritium production from neutron reactions with ^6Li and ^7Li nuclei were calculated along the central axis of a 0.60 m–diameter by 0.60 m–long assembly and four additional assemblies where sheets of stainless–steel type 304 and polyethylene were placed in front of the Li_2O to simulate first wall and coolant materials. The calculated data are compared with measured data obtained at the Fusion Neutron Source at the Japan Atomic Energy Research Institute. The calculated data reproduce the measured data in shape, but differ from the measured data by 10–20% in the case of ^6Li and as much as 30% at some spatial locations for the ^7Li tritium production.

1. INTRODUCTION

The nuclear performance of the blanket–shield assembly of a fusion reactor will have significant impact on the operation and cost of the reactor, so it is imperative that the nuclear analysis methods and data being used in the design of these assemblies be validated in advance of reactor design efforts. The U.S. Department of Energy (DOE) and the Japan Atomic Energy Research Institute (JAERI) are engaged in a cooperative fusion neutronics program directed at this validation process. In this program, integral experiments are being conducted at the Fusion Neutron Source (FNS) facility at JAERI by personnel from JAERI and the Argonne National Laboratory (ANL), and this experimental program is being complemented by analytic programs at JAERI, the University of California at Los Angeles (UCLA), and the Oak Ridge National Laboratory (ORNL).

In Phase I of this program, measured data, i.e., tritium production rates from the reactions of the 14 MeV neutrons in a lithium–oxide (Li_2O) assembly were obtained and have been compared with a variety of calculated results.[1,2] Additional details concerning the experiments and preliminary analytic results from the various institutions are also given in References 1 and 2. In this paper, calculated tritium production data obtained at ORNL using the Monte Carlo codes MORSE[3] and MCNP[4] are documented and compared with experimental results.

Details of the calculations and aspects of the experiment necessary for understanding the calculational details are given in Section 2. In Section 3, comparisons between the calculated and measured tritium production rates are presented and discussed.

2. DETAILS OF THE CALCULATIONS

The experimental facility for performing the tritium production measurements is shown in a plan view in Figure 1. Deuterons are raised to a kinetic energy of 350 keV using an accelerator located outside of the experiment test cell and directed into the cell where they focused onto a titanium–tritide target that is mounted in a rotating assembly. The deuterons react with the tritium nuclei to produce ≈14 MeV neutrons via the

$$\mathrm{D} + \mathrm{T} \rightarrow n + {}^{4}\mathrm{He} + 17.6\mathrm{MeV} \tag{1}$$

fusion reaction. The sensitive region of the target is located at the center of the experiment room at nominally 2.5 m from the interior wall surfaces and at 1.8 m above the floor and 2.7 m below the ceiling. The neutron yield from the target was measured using the associated particle method by counting ^{4}He (alpha) particles that are emitted into a well–defined solid angle with a solid state detector.

The dimensions of the experimental area and the concrete shielding are given in Figure 1. The interior surfaces of the room were coated with a 0.02 m–thick layer of mortar to reduce the accumulation of concrete dust in the room and, particularly, in the drive mechanisms of the rotating target assembly. The experiment port, in which the Li_2O assembly was placed, is approximately perpendicular to the deuteron beam–target axis. The deuteron beam enters the test cell at an angle of 10° with the normal to interior wall. The experiment port, which is formed with a stainless–steel pipe having a wall thickness of 0.045 m, has an inside diameter of 0.63 m over a length of 0.8 m and an inside diameter of 0.48 m over the remaining distance through the wall. The Li_2O was placed in steel containment trays having a cross section of 0.05×0.05 m^2 and a length of 0.61 m. These were arranged in a grid inside the port to form the experiment assembly. Trays having different structural material–to–Li_2O ratios were used to form the inner and outer regions of the Li_2O assembly. Insets 1 and 2 in Figure 1 show the details of the actual Li_2O assembly and the representation used in the calculations, respectively.

The axial distribution of the tritium production rates in the Li_2O was measured using Li–glass detectors enriched to 90% in ^{6}Li to obtain the tritium production with ^{6}Li nuclei via the $^6\mathrm{Li}+n \rightarrow {}^3\mathrm{H}+{}^4\mathrm{He}+4.78$ MeV reaction. These detectors were placed in the central Li_2O tray at several positions along the centerline of the assembly and were removed following exposure and analyzed in the laboratory. Tritium production from neutron reactions with ^{7}Li nuclei was inferred by using a small, spherical NE–213 scintillator detector to obtain the neutron spectra as a function of depth in the test assembly and folding these data with the energy–dependent cross section for the $^7\mathrm{Li} + \mathrm{n} \rightarrow {}^3\mathrm{H} + {}^4\mathrm{He} + \mathrm{n}' - 2.47$ MeV reaction to obtain tritium production data. Additional details of the experimental procedures may be found in References 1, 2, and 5–8.

The calculated tritium production rates were obtained using the Monte Carlo codes MORSE[3] and MCNP.[4] The experiment room concrete shielding, Li_2O assembly, and rotating target assembly were modeled in detail using the combinatorial geometry subroutines unique to each code system. All of the components were represented in sufficient detail to assure that the neutron transport was accurately treated in the calculations. In the calculations, the inner and outer Li_2O regions were modeled as co–axial cylinders as shown in Inset 2 of Figure 1. The inner Li_2O region was represented as a 0.127 m–radius cylinder surrounded by

a 0.07 m–thick SS.304 liner. The Li_2O and SS–304 was homogenized in each region in the appropriate Li_2O–to–steel ratios.

Neutrons produced in the D–T reactions in the titanium–tritide target are distributed in energy and angle with respect to the incident deuteron beam. This occurs since reactions take place at different energies as the deuterons slow down in the target. The probability that a deuteron of energy E_d reacts while traveling a distance dx in a target containing N_t tritium atoms per cm^3 is

$$P = N_t \int_0^{E_d} \sigma/(dE/dx) \tag{2}$$

where σ is the microscopic cross section for the $T(D,n)^4He$ reaction and dE/dx is the stopping power for deuterons in titanium–tritide. When the reaction cross section is a differential angular cross section, then P is the probability for emission per unit solid angle. In this work, Eq. (2) was solved using the procedures outlined in Reference 9 to obtain the neutron source data in multigroup energy format for use in the MORSE calculation. The procedure in Reference 9 was modified to obtain the energy–angle data in continuous energy format for use with MCNP.

Since the solid angle subtended by the front face of the Li_2O assembly is small (5×10^{-2} sr), biased neutron source sampling was used wherein 50% of the neutrons were directed into a "cone" having polar and aximuthal angles of $\pm 10°$ with respect to the direction from the point on the target where the D–T reactions occur to the center of the face of the Li_2O assembly. All other source neutrons were taken to be uniformly emitted everywhere else. The neutron source biasing scheme is shown schematically in Figure 2. The neutron emission into the polar angular interval was determined using the calculated energy–angle distribution discussed above. Neutron emission into the azimuthal angles was taken to be uniform.

The tritium production as a function of depth in the Li_2O assembly was calculated using collision density estimation in MORSE and track length estimation in MCNP. The collision density estimator used in the MORSE calculation is given by

$$T = (\sigma_i/\sigma_T) * \text{neutron weight}, \quad i = 6, 7 \tag{3}$$

where σ_i is the cross section for the tritium production from neutron reactions with ^6Li ($i = 6$) or ^7Li ($i = 7$) and σ_T is the neutron transport cross section in Li_2O. The ratio of these probabilities is multiplied by the weight of the neutron prior to initiation of the reaction. The spatial distribution of the tritium production was obtained by dividing the inner Li_2O region into 12 axial intervals. The interval dimensions selected to bracket the locations of the detectors used in the measurements and the locations of the detectors are summarized in Table 1.

The radiation transport calculations carried out using the MORSE code incorporated a 53–neutron energy group cross–section library obtained by collapsing the 174–neutron energy group VITAMIN–E data library[10] (ENDF/B–V). The VITAMIN–E library was created as a general purpose cross–section data set for fusion neutronics and other radiation analysis problems. The fine group library was collapsed using the ANISN code[11] using forward emitted (0 to 40–deg) neutron energy–angle data as the energy weighting function. The angular dependence of the cross sections for all nuclei was approximated using a P_3 legendre expansion. The energy boundaries of the collapsed data library are given in Table 2. Also given in the table are cross sections for the tritium production from neutron reactions with ^6Li and ^7Li nuclei.

TABLE 1

Detector Locations and Monte Carlo Estimator Cell Dimensions[a]

Detector No.	^{6}Li Detectors	^{7}Li Detectors	Estimator Interval Thickness	Estimator[b] Volume
	(cm)	(cm)	(cm)	(cm^3)
			0.0	
1	0.25			1558.62
			0.50	
2	1.26	1.60		4738.20
			2.06	
3	2.53			3179.58
			3.04	
4	3.81	3.88		4800.55
			4.58	
5	5.06			4426.48
			6.00	
6	7.61			6234.48
			8.00	
7	10.12	11.47		12468.96
			12.00	
8	15.20			18703.44
			18.00	
9	20.24	21.59		21820.68
			25.00	
10	30.30	31.71		31172.45
			35.00	
11	40.45	41.85		31172.45
			45.00	
12	55.72			49439.43
			60.86	

[a]Measured from the front face of the Li_2O Assembly.
[b]Scoring radius—31.5 cm.

The MCNP calculations were performed using Version 3 of the code that is maintained at the National Magnetic Fusion Energy Computer Center at Lawrence Livermore National Laboratory. ENDF/B–V transport cross sections were taken from the RMCCS13, ENDF5P3, and ENDF5V3 data files.[4] The composition of the materials used in the calculations are given in Table 3.

In both calculations, Russian roulette and particle splitting were used to reduce the variance in the estimated results.

TABLE 2

53–Neutron Energy Group Structure and Tritium Breeding Cross Sections

Neutron	Upper Energy	^{6}Li Breeding	^{7}Li Breeding	Neutron	Upper Energy	^{6}Li Breeding	^{7}Li Breeding
	ev	b	b		ev	b	b
1	17.33+06[a]	0.0193	0.2468	28	6.081+05	0.3386	
2	15.68+06	0.0239	0.2869	29	4.978+05	0.4881	
3	14.92+06	0.0246	0.2929	30	3.688+05	0.9891	
4	14.55+06	0.0253	0.2985	31	2.985+05	1.5127	
5	14.19+06	0.0260	0.3039	32	2.972+05	2.4440	
6	13.84+06	0.0266	0.3091	33	1.832+05	0.9060	
7	13.50+06	0.0273	0.3149	34	1.111+05	0.6553	
8	12.84+06	0.0294	0.3304	35	6.737+04	0.7194	
9	12.21+06	0.0323	0.3419	36	4.087+04	0.8693	
10	11.05+06	0.0359	0.3542	37	2.479+04	0.9860	
11	10.00+06	0.0402	0.3636	38	2.359+04	1.1017	
12	9.048+06	0.0454	0.3707	39	1.503+04	1.3824	
13	8.187+06	0.0506	0.3751	40	4.119+03	1.7608	
14	7.408+06	0.0598	0.3714	41	5.531+03	2.2521	
15	6.065+06	0.0752	0.2525	42	3.354+03	2.8847	
16	4.966+06	0.0956	0.0753	43	2.035+03	3.7109	
17	4.066+06	0.1122	0.0158	44	1.234+03	4.7769	
18	3.679+06	0.1436	0.0010	45	7.485+01	6.1240	
19	2.725+06	0.1925		46	4.540+02	7.8654	
20	2.365+06	0.2025		47	2.754+02	10.102	
21	2.307+06	0.2051		48	1.670+02	12.978	
22	2.231+06	0.2102		49	1.013+02	16.660	
23	1.653+06	0.2141		50	6.144+01	21.404	
24	1.353+06	0.2265		51	3.726+01	31.860	
25	8.629+05	0.2484		52	1.067+01	76.377	
26	8.208+05	0.2584		53	4.139−01	526.5	
27	7.427+05	0.2842			1.000−5		

TABLE 3

Composition of Materials Used in the Calculation

	Composition (at./cm × b)						
Element	Air	SS–304	Water	Concrete	Mortar	Inner Li_2O	Outer Li_2O
Hydrogen			6.69×10^{-2}	9.42×10^{-3}	7.97×10^{-3}		
^{6}Li						4.24×10^{-3}	3.86×10^{-3}
^{7}Li						5.29×10^{-2}	4.81×10^{-2}
Carbon				7.42×10^{-4}			
Nitrogen	3.88×10^{-5}						
Oxygen	1.04×10^{-5}		3.34×10^{-2}	4.31×10^{-2}	4.31×10^{-2}	2.85×10^{-2}	2.60×10^{-2}
Sodium				5.08×10^{-4}	7.85×10^{-4}		
Magnesium				4.68×10^{-4}	3.82×10^{-4}		
Aluminum				1.94×10^{-3}	2.63×10^{-3}		
Silicon				1.13×10^{-2}	1.48×10^{-2}		
Potassium				3.34×10^{-4}	5.29×10^{-4}		
Calcium				3.71×10^{-3}	2.56×10^{-3}		
Chromium		1.74×10^{-2}				2.56×10^{-4}	1.40×10^{-4}
Iron		6.17×10^{-2}		6.81×10^{-4}	5.86×10^{-4}	9.22×10^{-4}	5.04×10^{-4}
Nickel		8.11×10^{-3}				1.12×10^{-4}	6.18×10^{-5}
Manganese						2.23×10^{-5}	1.22×10^{-5}
		Copper		Aluminum		Iron	
		8.46×10^{-2}		6.00×10^{-2}		8.47×10^{-2}	

3. DISCUSSION OF RESULTS

The tritium production was measured and calculated for five configurations: the Li_2O reference assembly shown in Figure 1 and four additional configurations where layers of SS–304 and/or polyethylene (PE) in various thicknesses and combinations were placed in front of the Li_2O reference assembly. The purpose of including the SS–304 and PE layers was to assess the impact on the tritium production of a typical first wall material (SS–304) and a coolant channel using PE as a simulator for hydrogenous cooling materials. The experimental configurations, dimensions, and materials are summarized in Table 4.

TABLE 4

Experimental Configurations Used for the Tritium Production Measurements

Configuration	SS–304	Polyethylene	Li_2O Assembly
	(cm)	(cm)	(cm)
1	—	—	61.0
2	0.5	—	61.0
3	1.5		61.0
4	0.5	0.5	61.0
5	1.5	1.5	61.0

The measured and calculated tritium production from the reactions of the source neutrons with ^{6}Li nuclei in the experimental configurations given in Table 4 are compared in Figures 3–7. In the figures, the open circles are the measured data and the solid and dashed histograms are the calculated tritium production data obtained from MORSE and MCNP, respectively. The solid curve connecting the measured data points is included only to show the trend in the measured tritium production and has not been fitted to the data. The experimental uncertainties in the measured data are small ($\approx$2–3%) and correspond, approximately, to the size of the circles. The error bars on the histograms indicate plus and minus one standard deviation in the estimated tritium production obtained with the MORSE and MCNP codes. The calculations were run using source populations sufficient to achieve approximately $\pm$10% standard deviation in the tritium production in the front of the Li_2O assembly. The measured and calculated data are normalized to one source neutron and the ^{6}Li nuclide density in Li_2O.

The spatial distribution of the tritium production in ^{6}Li is essentially the same for all of the experimental assemblies. The tritium production decreases by approximately an order of magnitude in the first 10 cm of the Li_2O and then decreases more gradually over the remaining thickness. The same behavior is observed in the calculated data.

The ^{6}Li tritium production calculated using the MORSE code is in reasonably good agreement with the measured data over the first 10 cm in the Li_2O assembly for all of the experimental configurations. The MCNP code, on the other hand,

over–predicts the measurement at very shallow depths in the Li_2O ($\leq$2.5 cm) and then falls into reasonable agreement at depths between 2.5 and ~15 cm. Both calculations over–predict the tritium production from a depth of 20 cm to the rear of the assembly. The calculated data are systematically higher than the measured data albeit they agree with each other, within statistics, at distances into the blanket between 20 and ~45 cm. MCNP consistently over–predicts both the MORSE and measured data at the rear of the Li_2O assembly.

The calculated–to–experimental (C/E) ratios for the MORSE data are shown in Figures 8–12. The MCNP data were not included in these comparisons to minimize confusion in the plotted results and since the C/E ratios show essentially the same trend. The error bars on the data in Figures 8–12 reflect the range in the C/E values imposed by the standard deviations in the calculated data. For the preponderant number of points, the C/E ratio indicates that MORSE reproduces the measurement within nominally 20%. The largest differences between the estimated and measured tritium production data occur at distances greater than 20 cm into the breeding assembly.

The measured and calculated tritium production rates from neutron reactions with ^{7}Li are compared in Figures 13–17. The data points and the histograms have the same meaning as discussed above. These data have also been normalized to one source neutron but are divided by the ^{7}Li nuclide density.

The calculated ^{7}Li tritium production as a function of distance in the Li_2O assembly reproduce the measured data in shape but not in magnitude in all of the experimental configurations except for the case where 0.5 cm of stainless–steel precedes the Li_2O assembly (Figure 14). The MORSE and MCNP data consistently over–predicts the measurements. However, this may arise, in part, from the selection of the estimator interval dimensions used in the collision density and track length estimation in the two codes. The interval dimensions were selected to bracket the detector locations for the ^{6}Li assembly particularly since both sets of calculated data are in reasonably good agreement with each other.

Finally, for completeness, the calculated–to–experimental ratios from the ^{7}Li tritium production data are compared in Figures 18–22. The C/E values are, in some cases and for specific detector locations, larger than desired and probably due to the selection of the histograms interval size.

The MORSE and the MCNP codes reproduce both the ^{6}Li and ^{7}Li measurements in shape. Differences in magnitude may be attributed to a number of causes. The geometry of the experiment challenges a Monte Carlo analysis. The volume of the Li_2O assembly is small compared to the volume of the concrete that forms the experimental room. The fraction of source neutrons reaching the surface of the Li_2O assembly is small so biasing techniques were imposed to achieve reasonable statistics in the estimation of the tritium breeding. As in all analyses where biasing is used, the results may be, in part, influenced by the procedures used to sample from the neutron source distribution.

Additionally, differences between the calculated and measured results may arise, at least in the case of the MORSE analysis, from the use of multigroup cross–section data. Representing the ^{6}Li tritium production thermal cross section in this format may lead to the rather large differences in the MORSE and MCNP predictions of the ^{6}Li tritium production at the front of the Li_2O assembly. The estimates of the ^{6}Li tritium production obtained in this study using the MCNP code are reasonably consistent with those obtained by the UCLA group using the same code.[1]

However, different procedures were used to sample from the neutron source and to model the experimental facility. In this work, the neutrons were sampled from the angle–energy distribution at the target. Biasing was used to direct more neutrons in the vicinity of the Li_2O assembly thereby minimizing the tracking time of neutron migration in regions of the geometry where their contributions to the tritium production would be small. Since the experiment room was modeled in reasonable detail, contributions to the tritium production from neutrons scattered from the room walls to the Li_2O assembly were accounted for directly. In the UCLA analysis,[1] the neutron source was represented by direct and indirect components. The direct component was represented by an anisotropic point source at the target and accounted for neutrons emitted into 13 angular intervals covering the face of the Li_2O assembly. The indirect source is an isotropic plane source that was used to account for neutrons emitted from the experiment room walls. Since this representation for the source was used, only the Li_2O and a small region of the concrete surrounding the Lithium assembly were modeled. Details of the UCLA calculations may be found in Reference 12.

The differences in the source sampling procedure and the representation of the experiment room geometry used at ORNL and UCLA may account for some of the differences observed among the calculated results obtained at the two institutions.

Considerable analysis of these experiments have been carried out by JAERI and UCLA analysts using a variety of Monte Carlo and discrete ordinates codes with generally the same results as achieved here: the C/E ratios are larger than optimum, where optimum is defined as 10% or less. However, considering the complexity of the experiment and that it does not represent the best choice for an integral experiment configuration, the results achieved here, as well as those obtained by JAERI and UCLA researchers, is quite favorable and suggests that reasonable estimates of tritium breeding in reactor geometries may be achieved with Monte Carlo methods.

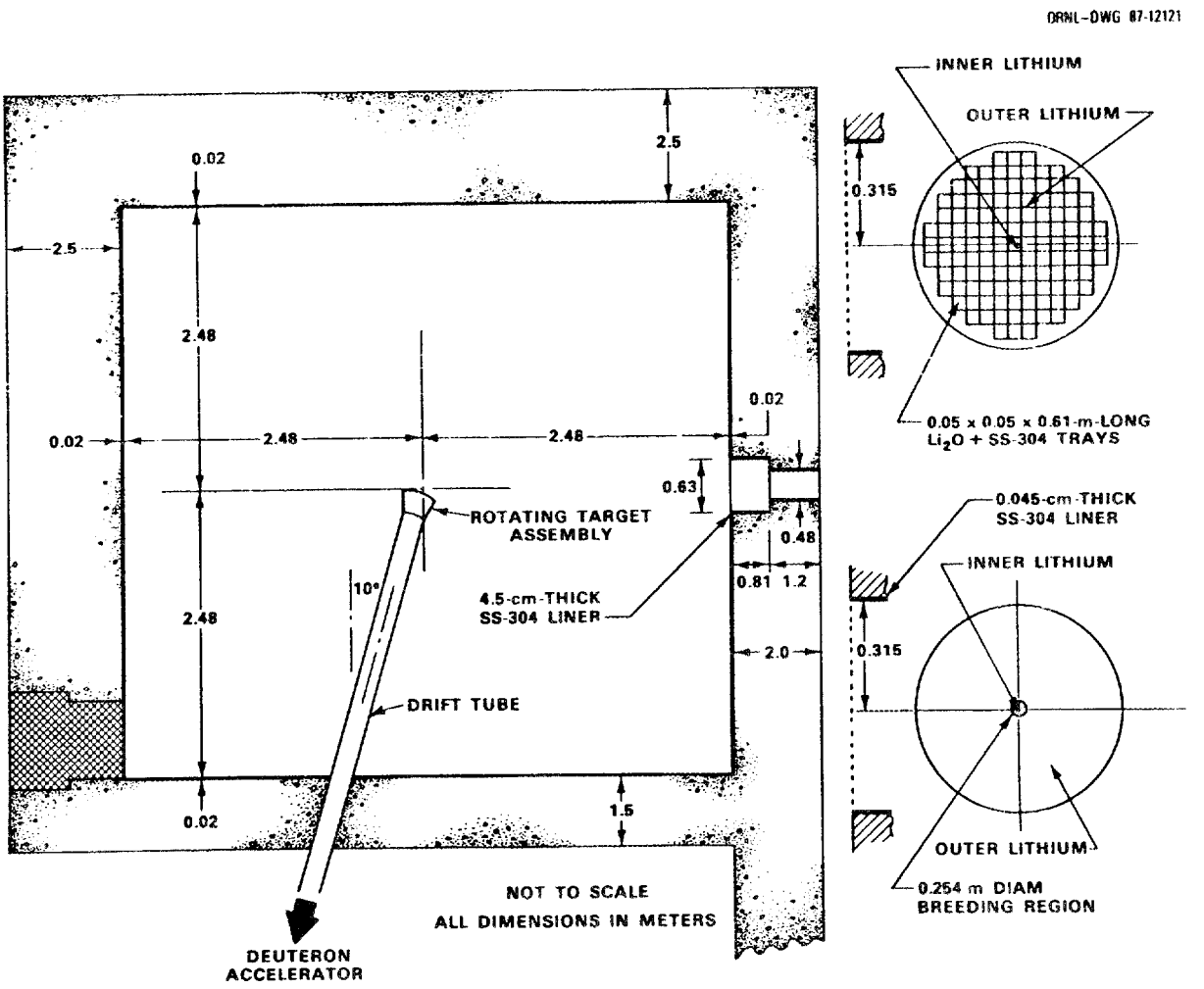

Figure 1. Plan View of the Experiment Room.

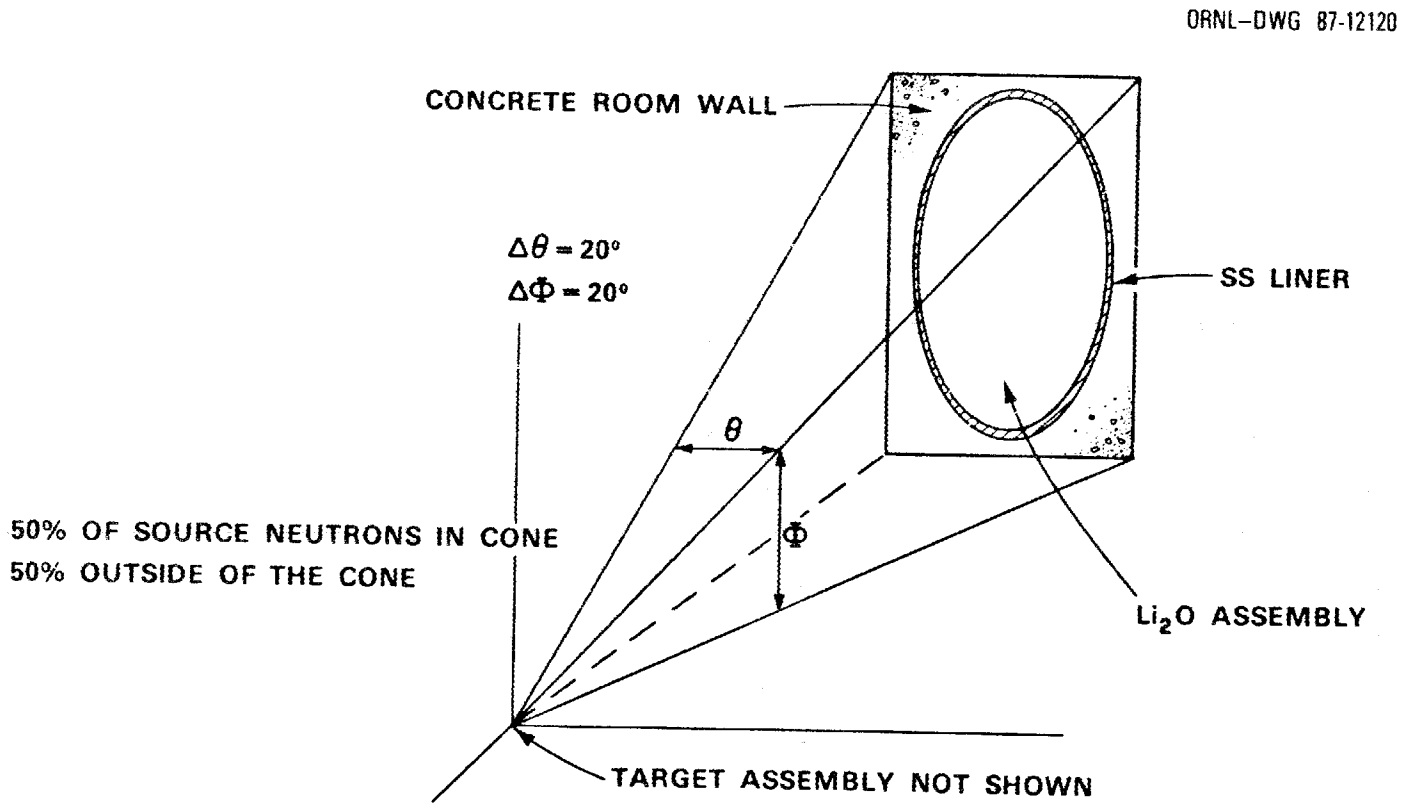

Figure 2. Schematic of the Neutron Biasing Scheme.

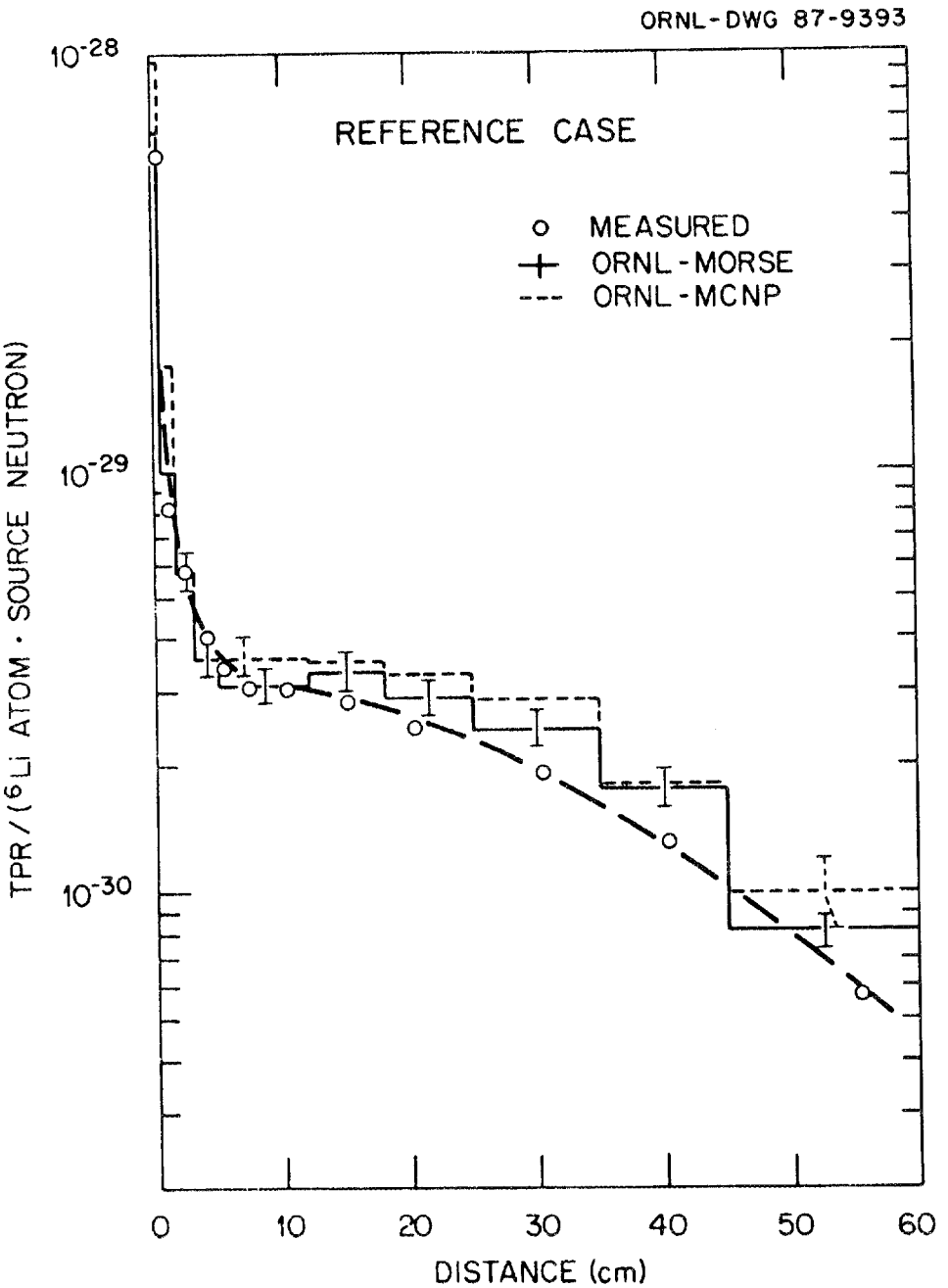

Figure 3. ^{6}Li Tritium Production vs Distance in the Li_2O Assembly–Reference Case.

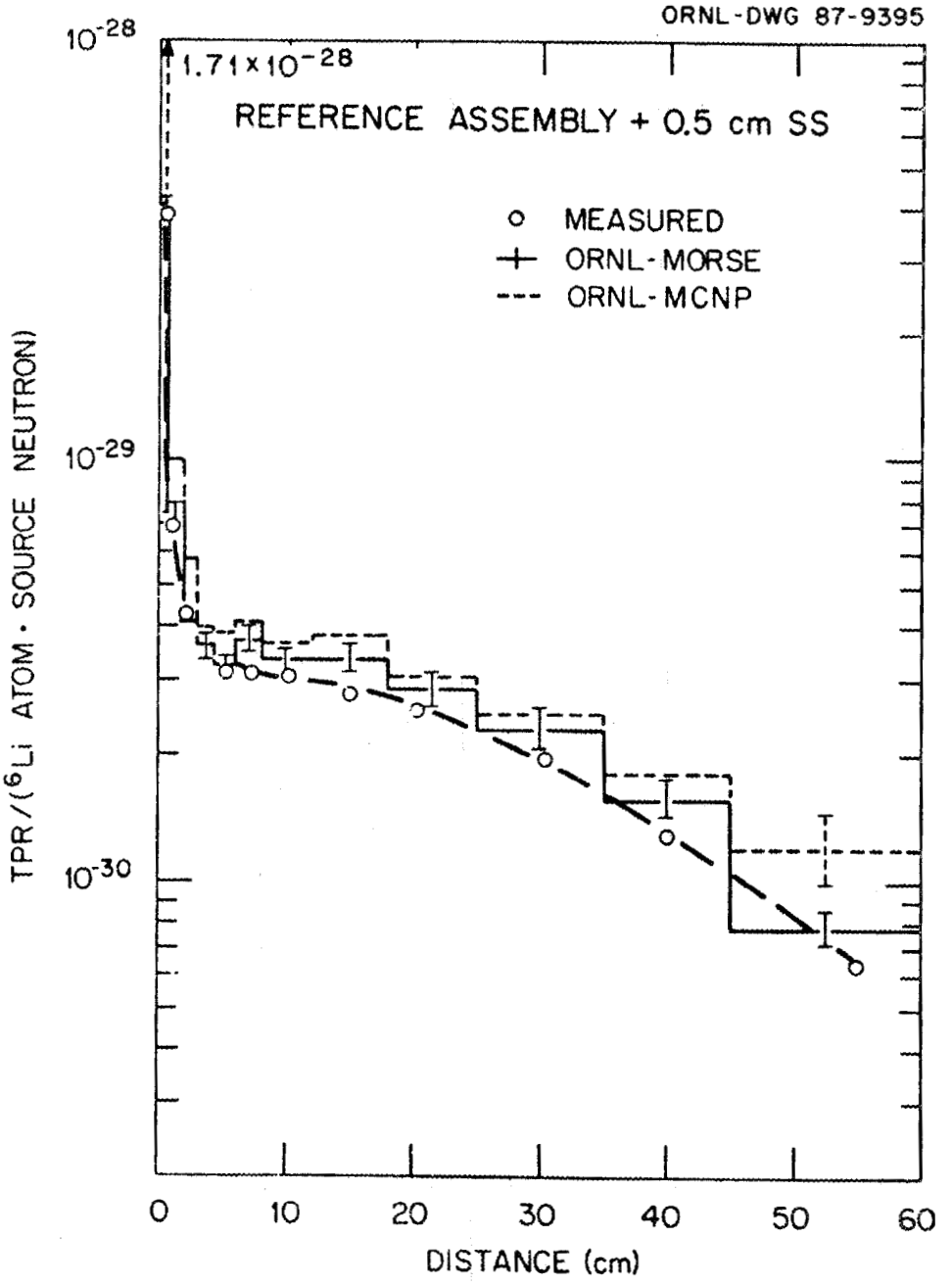

Figure 4. ^{6}Li Tritium Production vs Distance in the Li_2O Assembly with 0.5 cm–thick SS–304.

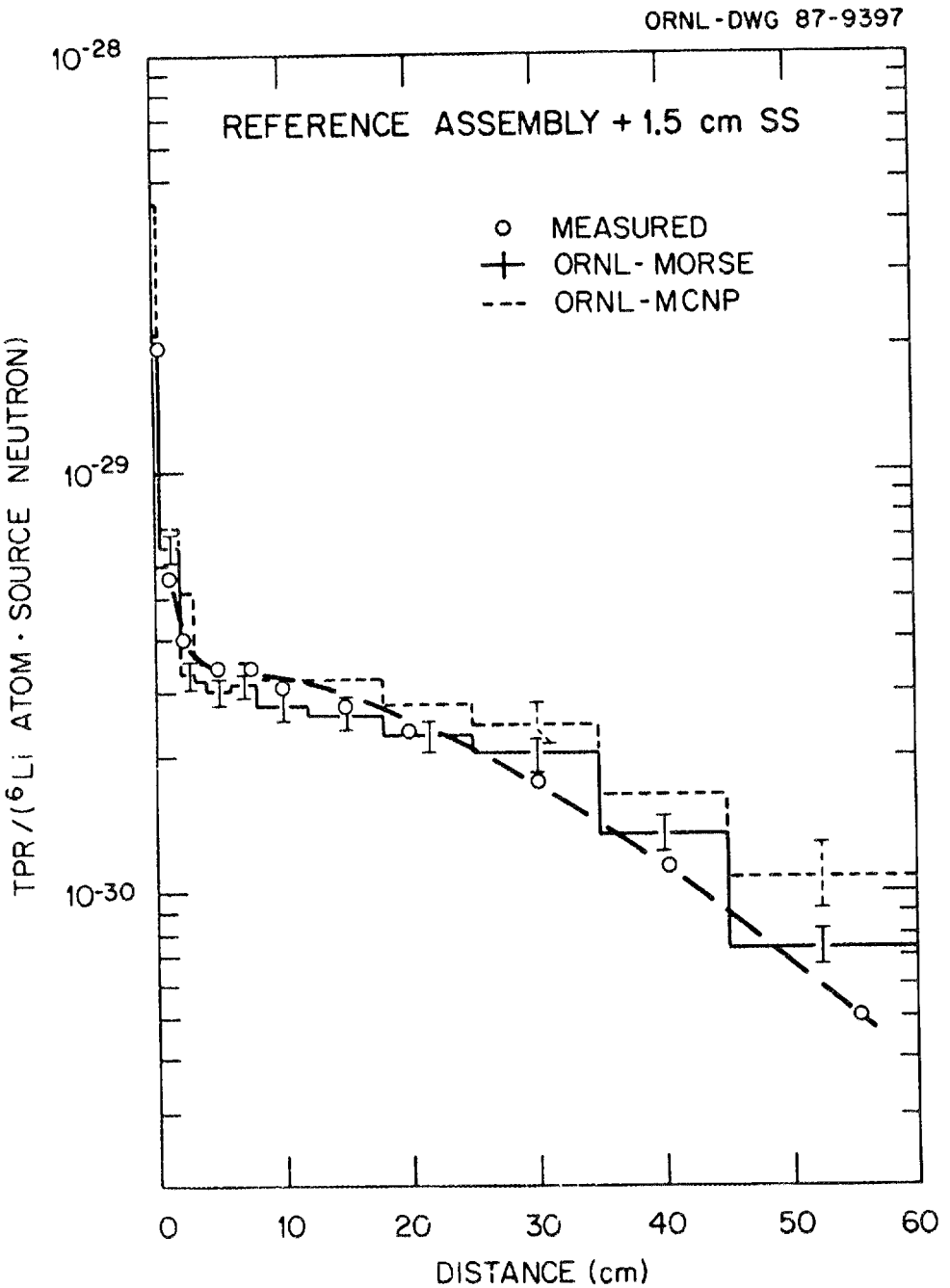

Figure 5. ^{6}Li Tritium Production vs Distance in the Li_2O Assembly with 1.5 cm–thick SS–304.

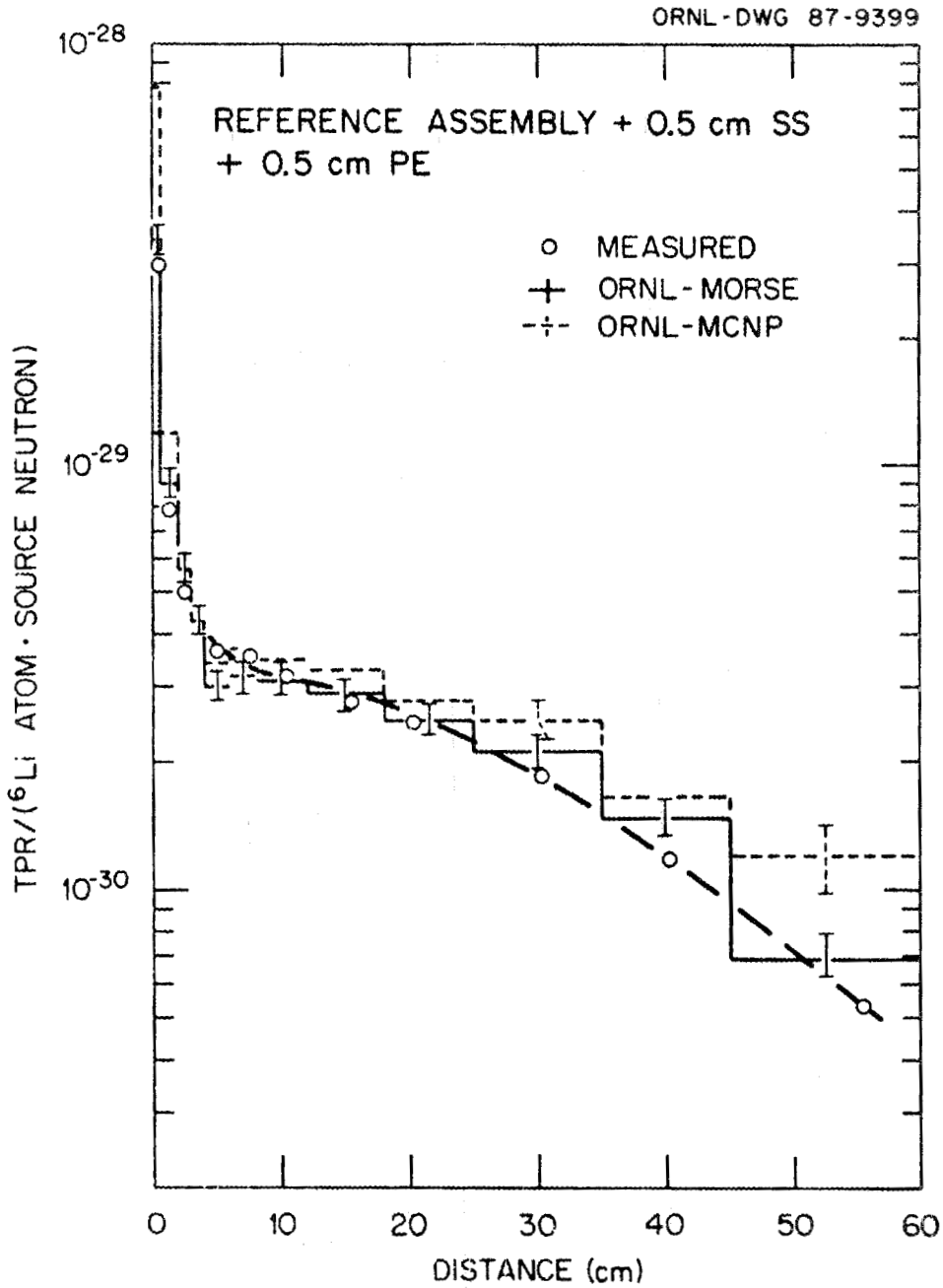

Figure 6. ^{6}Li Tritium Production vs Distance in the Li_2O Assembly with 0.5 cm–thick SS–304 and 0.5 cm–thick Polyethylene.

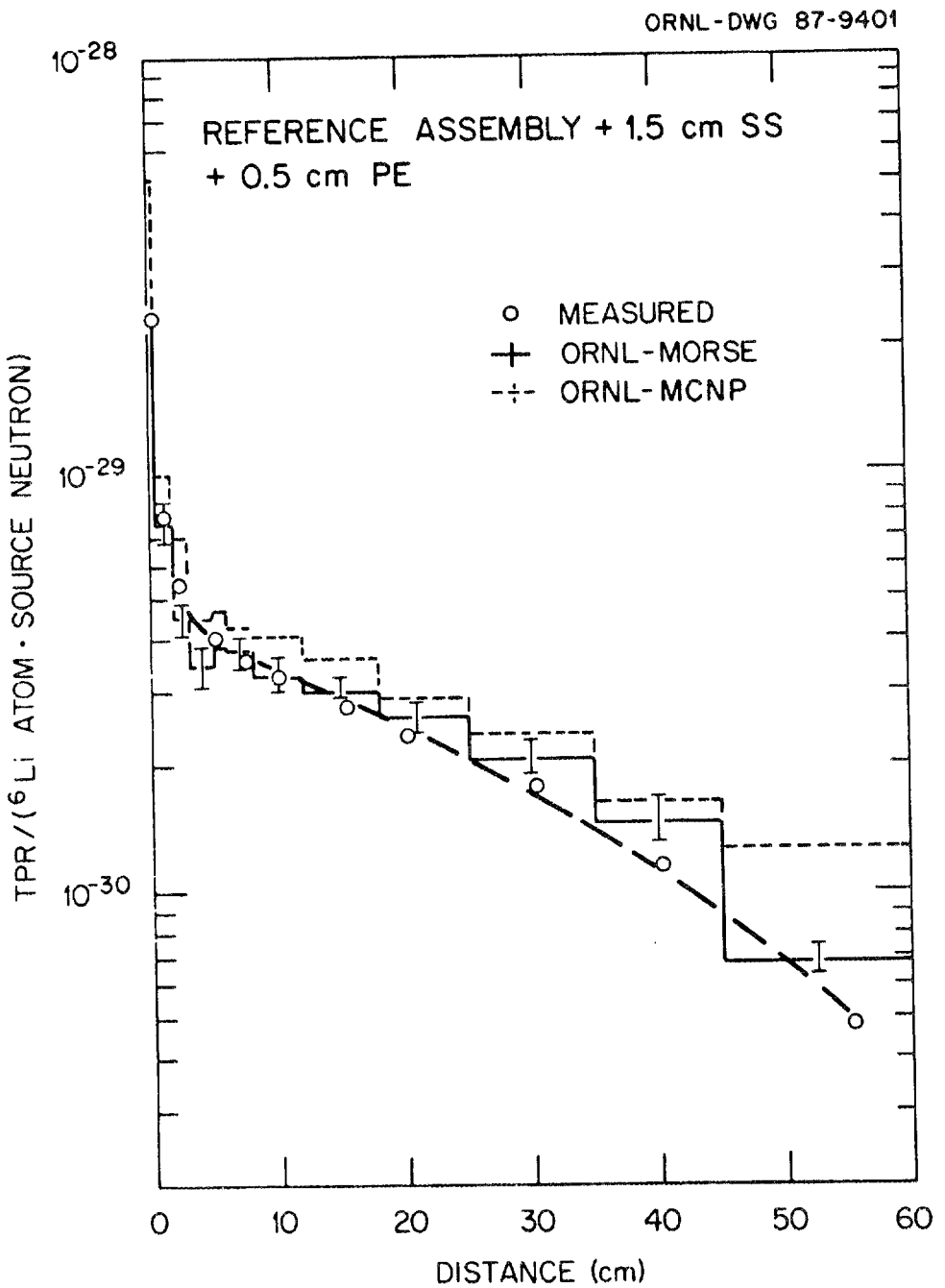

Figure 7. ^{6}Li Tritium Production vs Distance in the Li_2O Assembly with 1.5 cm–thick SS–304 and 0.5 cm–thick Polyethylene.

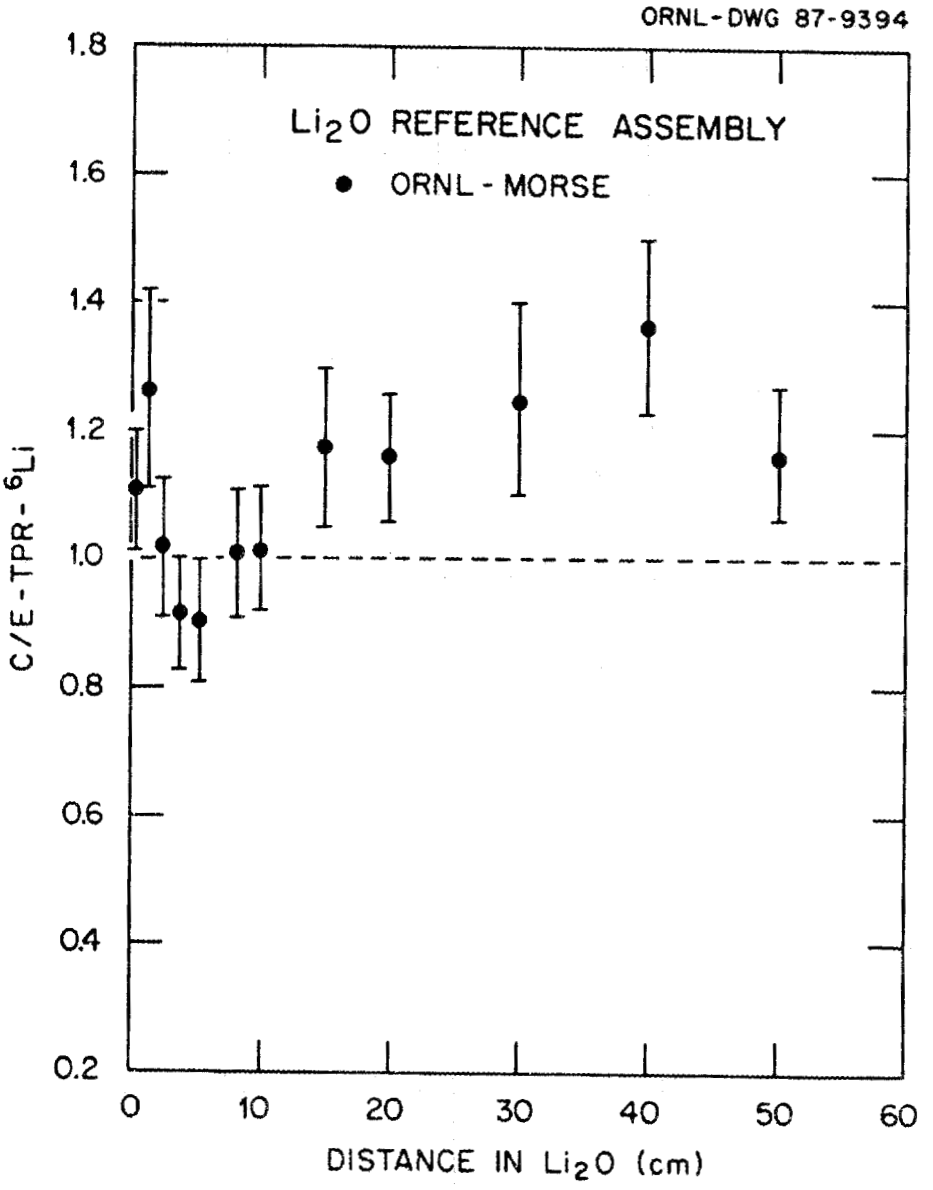

Figure 8. Calculated-to-Experimental Ratio for ^{6}Li Tritium Production vs Distance in the Li_2O Assembly-Reference Case.

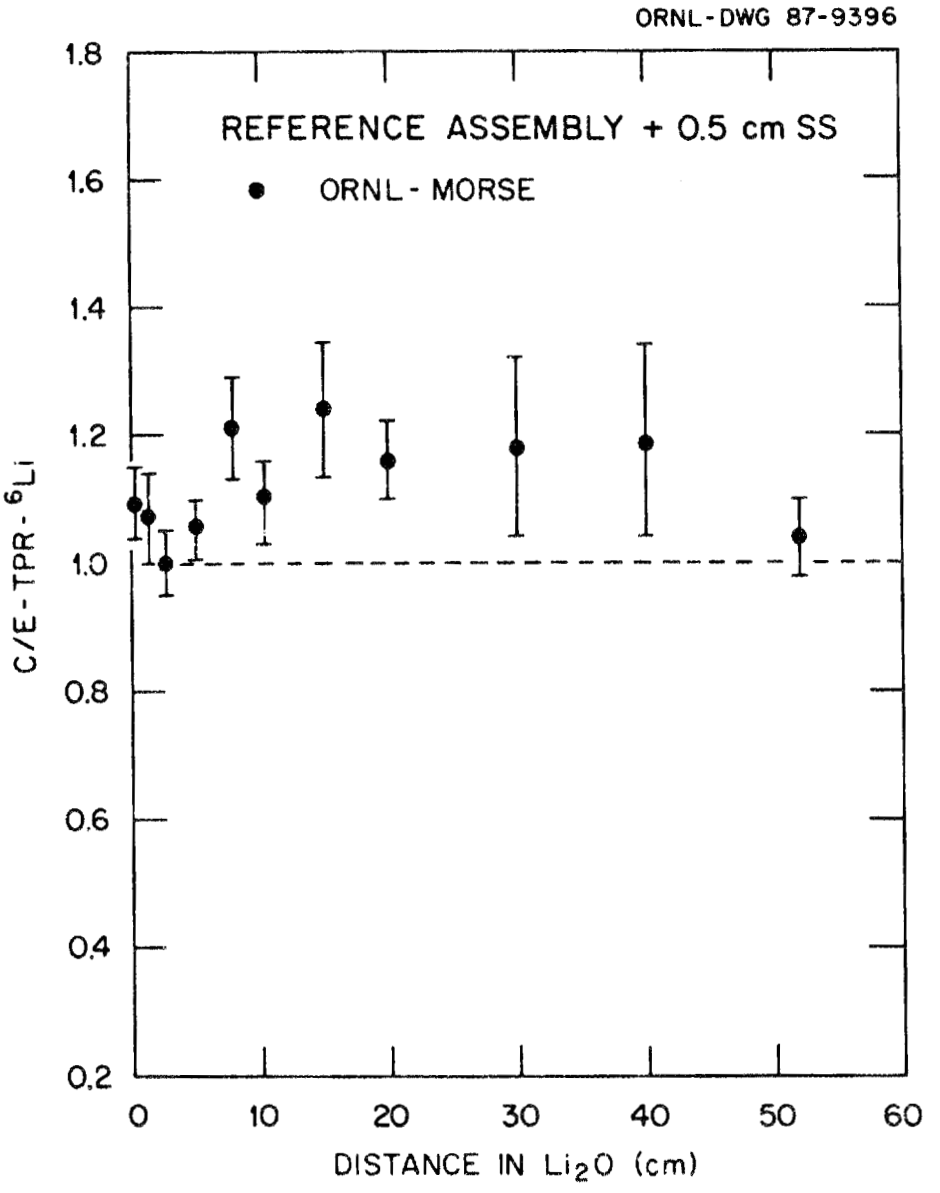

Figure 9. Calculated–to–Experimental Ratio for ^{6}Li Tritium Production vs Distance in the Li_2O Assembly with 0.5 cm–thick SS–304.

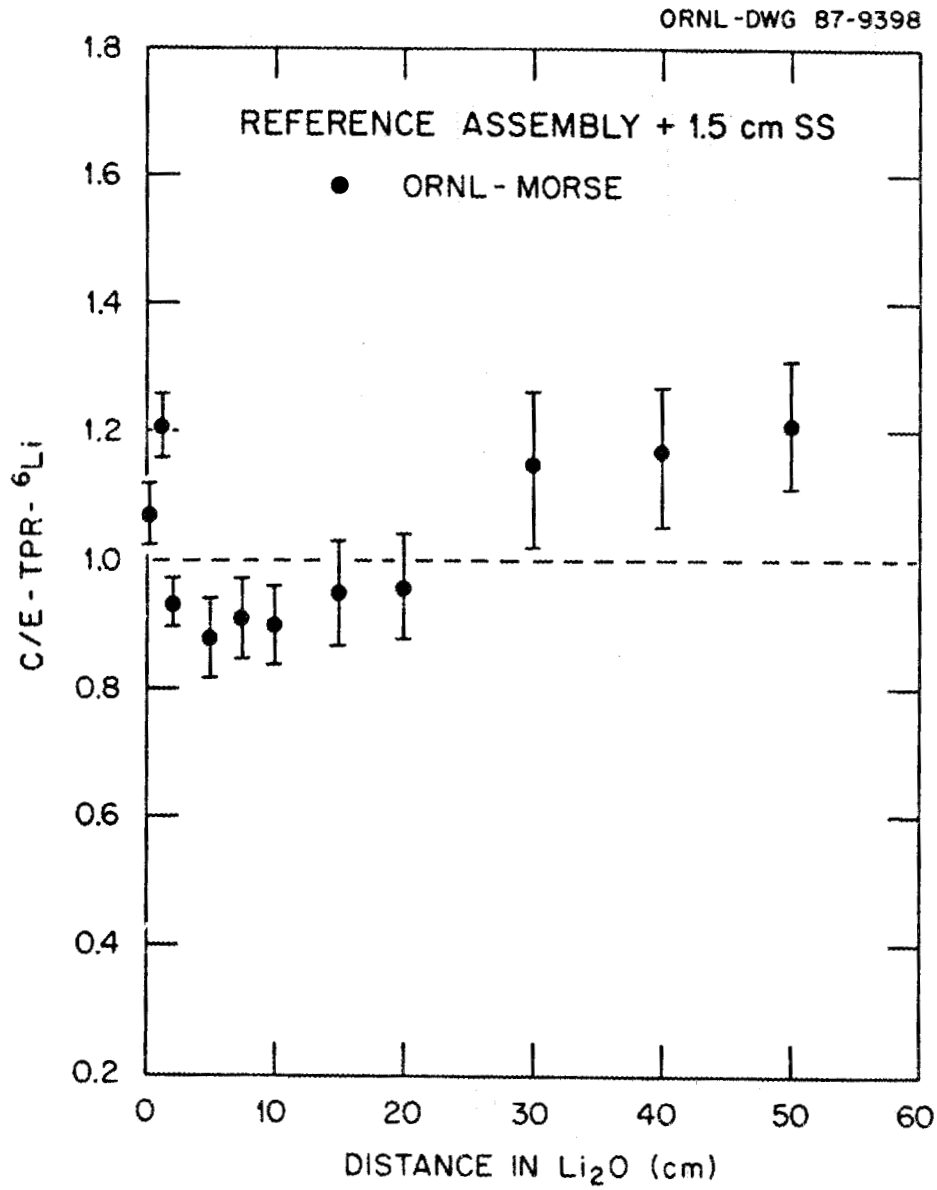

Figure 10. Calculated–to–Experimental Ratio for ^{6}Li Tritium Production vs Distance in the Li_2O Assembly with 1.5 cm–thick SS–304.

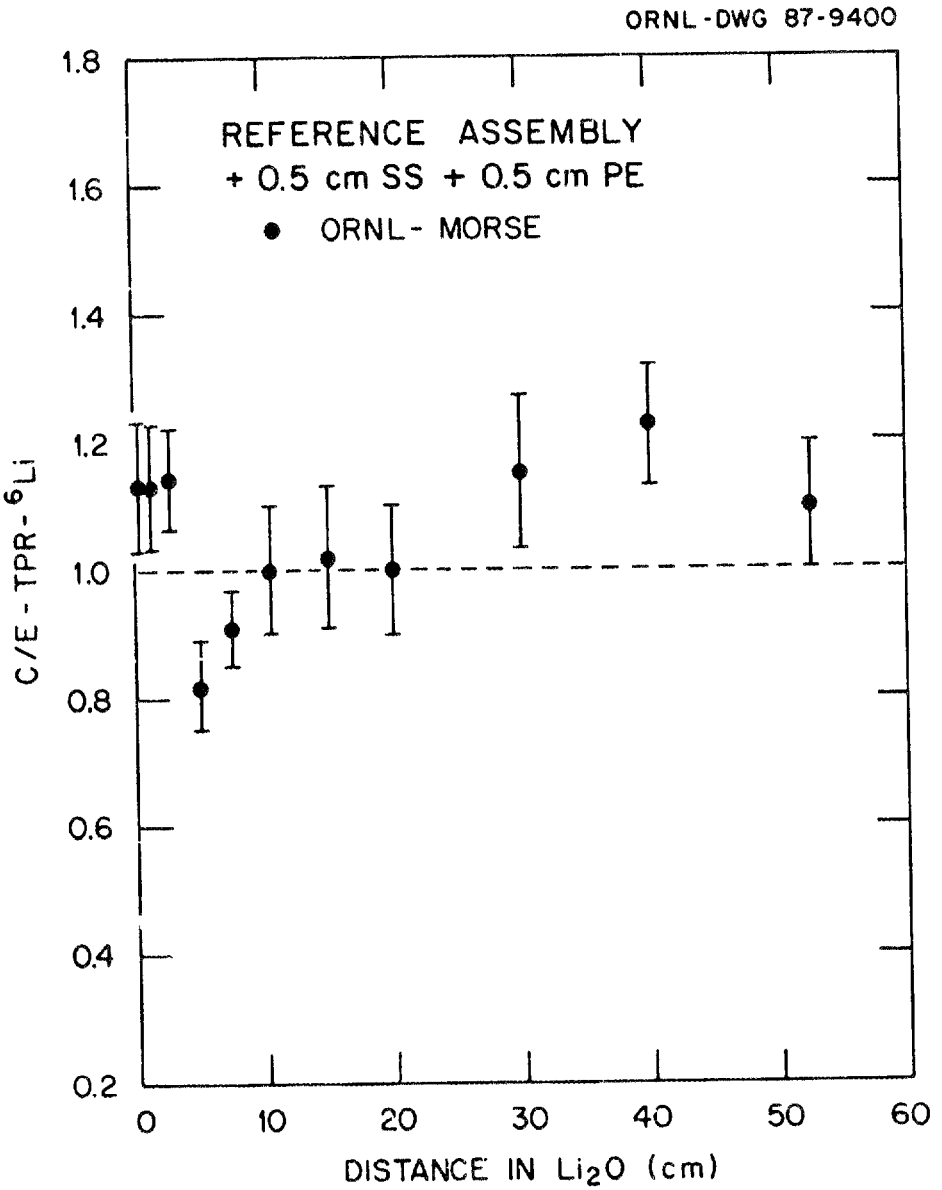

Figure 11. Calculated–to–Experimental Ratio for ^{6}Li Tritium Production vs Distance in the Li_2O Assembly with 0.5 cm–thick SS–304 and 0.5 cm–thick Polyethylene.

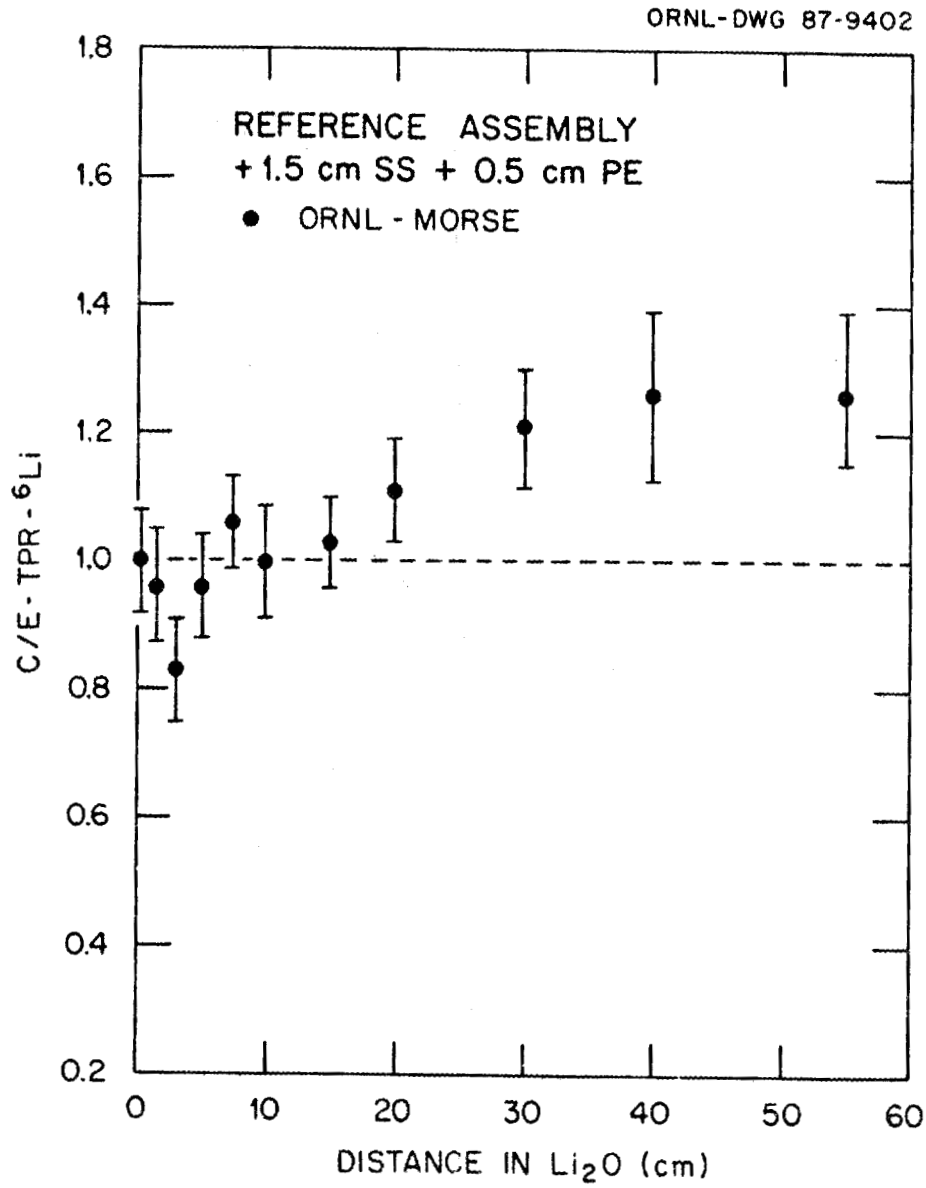

Figure 12. Calculated–to–Experimental Ratio for ^{6}Li Tritium Production vs Distance in the Li_2O Assembly with 1.5 cm–thick SS–304 and 0.5 cm–thick Polyethylene.

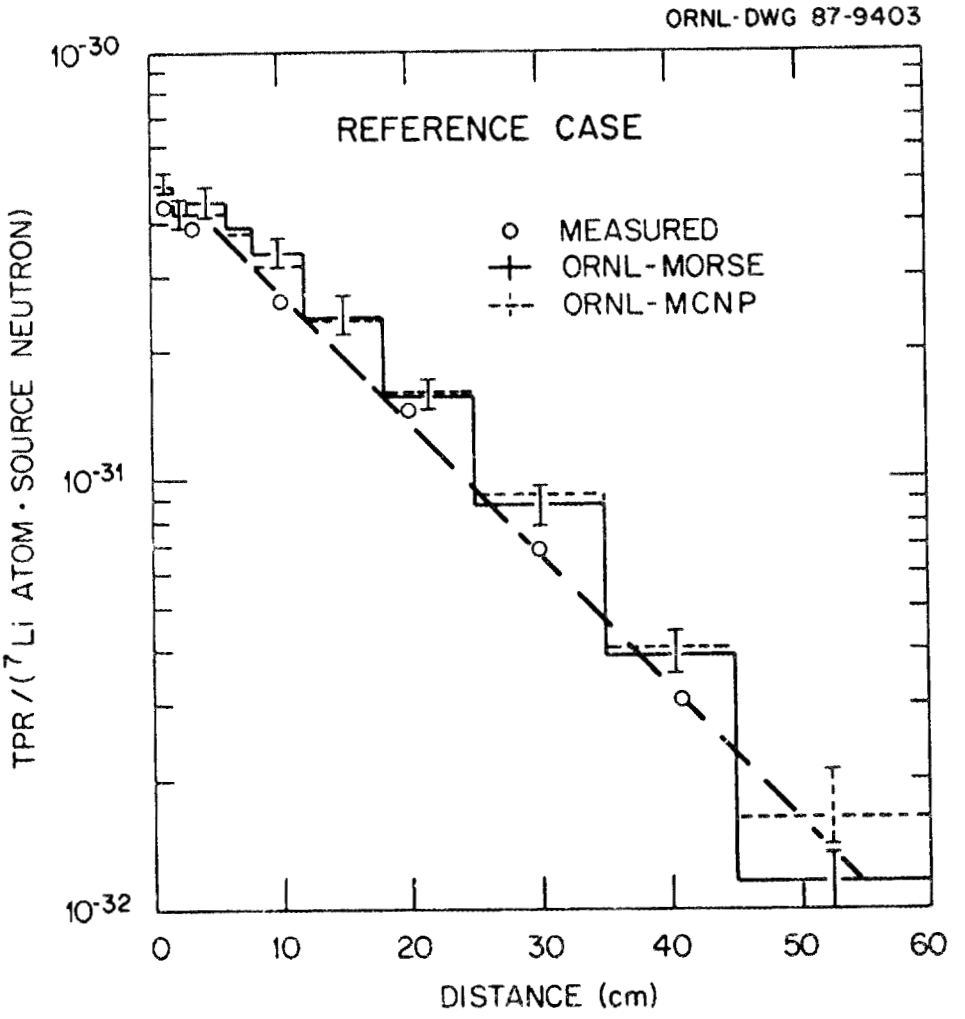

Figure 13. ^{7}Li Tritium Production vs Distance in the Li_2O Assembly–Reference Case.

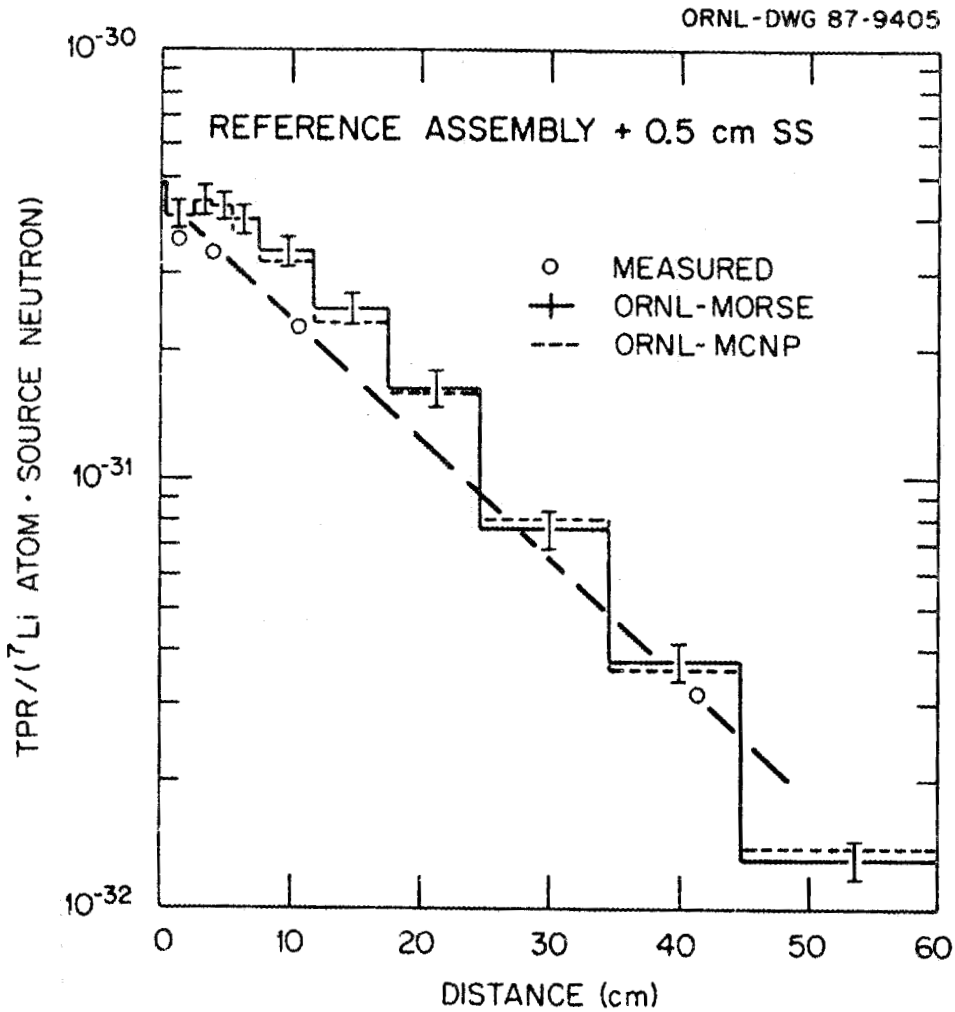

Figure 14. ^{7}Li Tritium Production vs Distance in the Li_2O Assembly with 0.5 cm–thick SS–304.

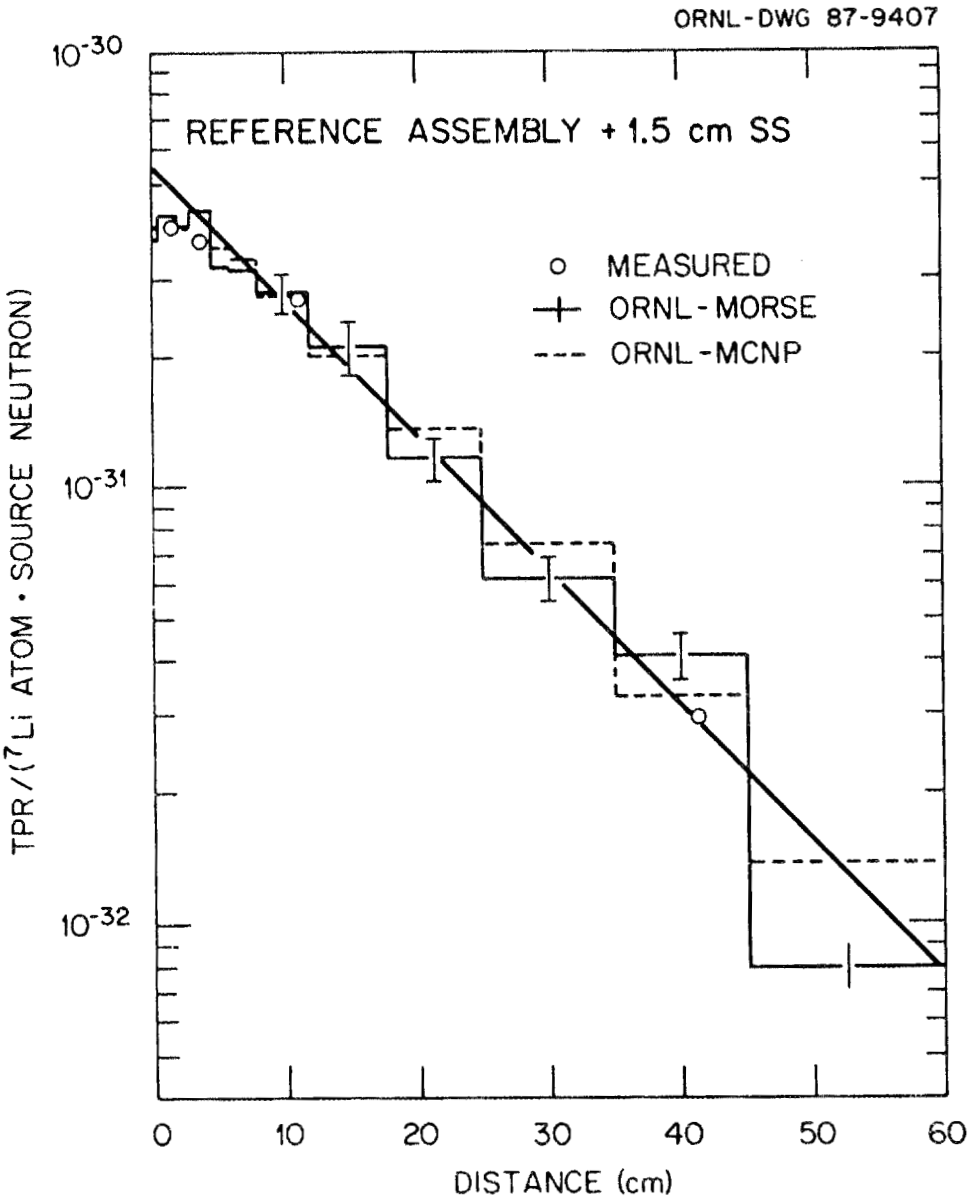

Figure 15. ^{7}Li Tritium Production vs Distance in the Li_2O Assembly with 1.5 cm–thick SS–304.

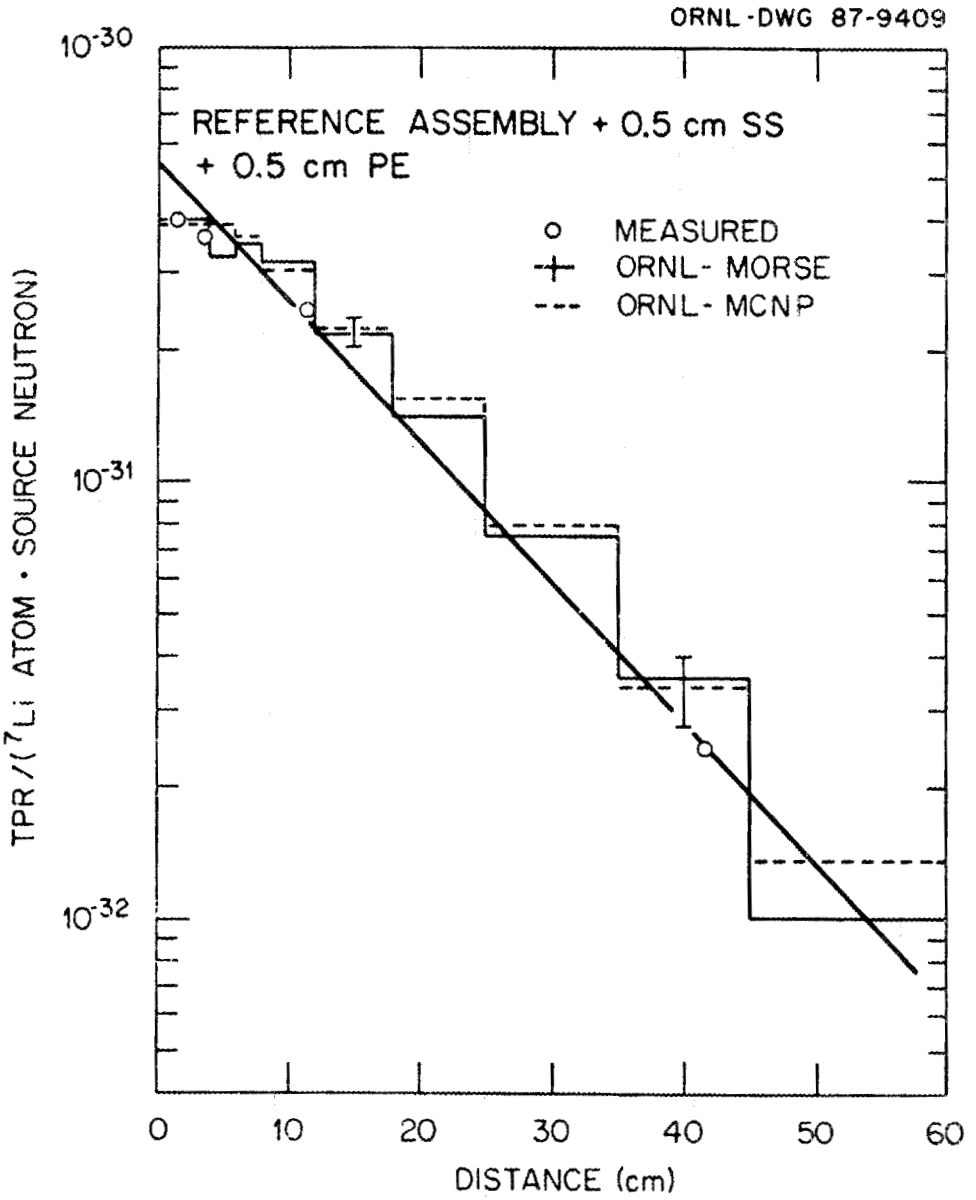

Figure 16. ^{7}Li Tritium Production vs Distance in the Li_2O Assembly with 0.5 cm-thick SS-304 and 0.5 cm-thick Polyethylene.

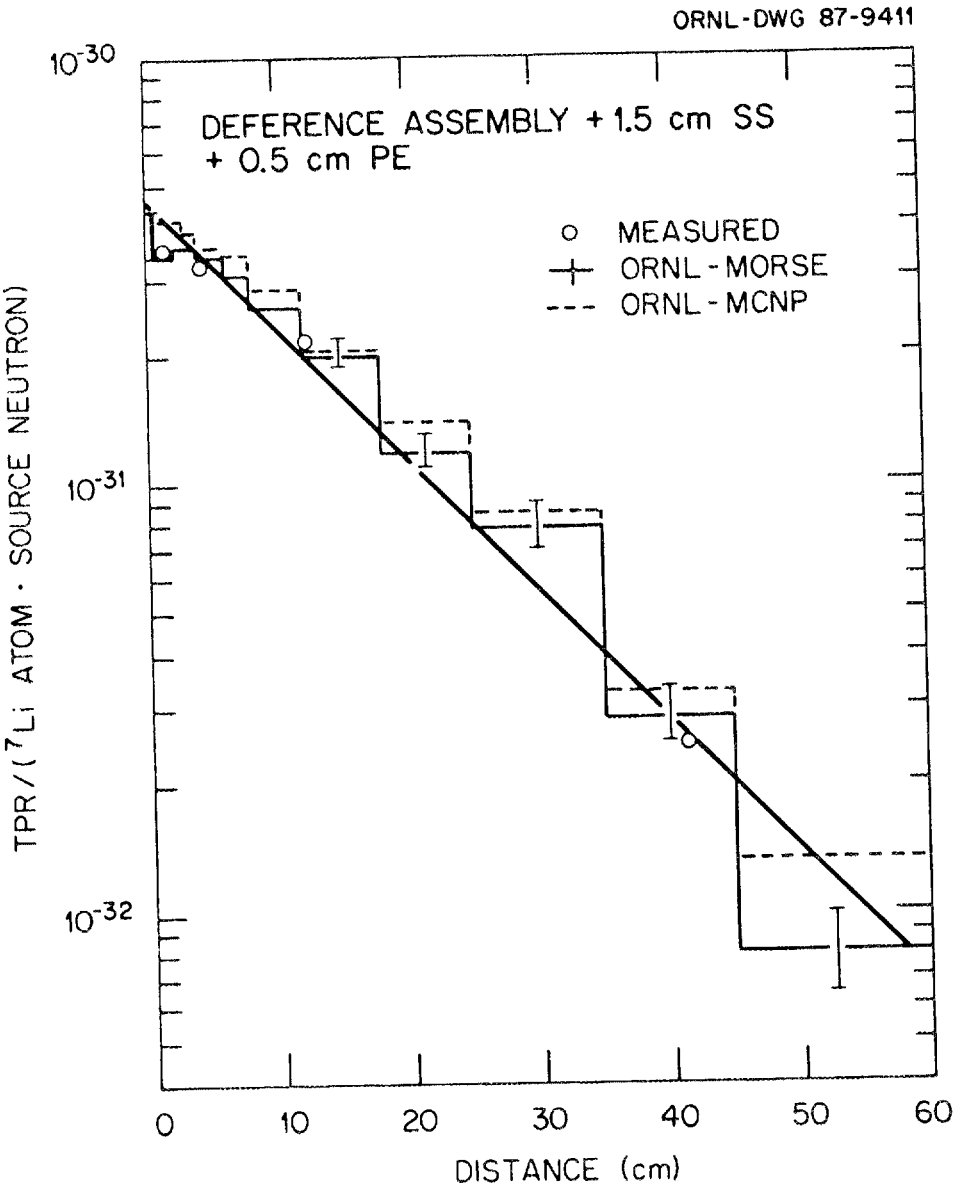

Figure 17. ^{7}Li Tritium Production vs Distance in the Li_2O Assembly with 1.5 cm–thick SS–304 and 0.5 cm–thick Polyethylene.

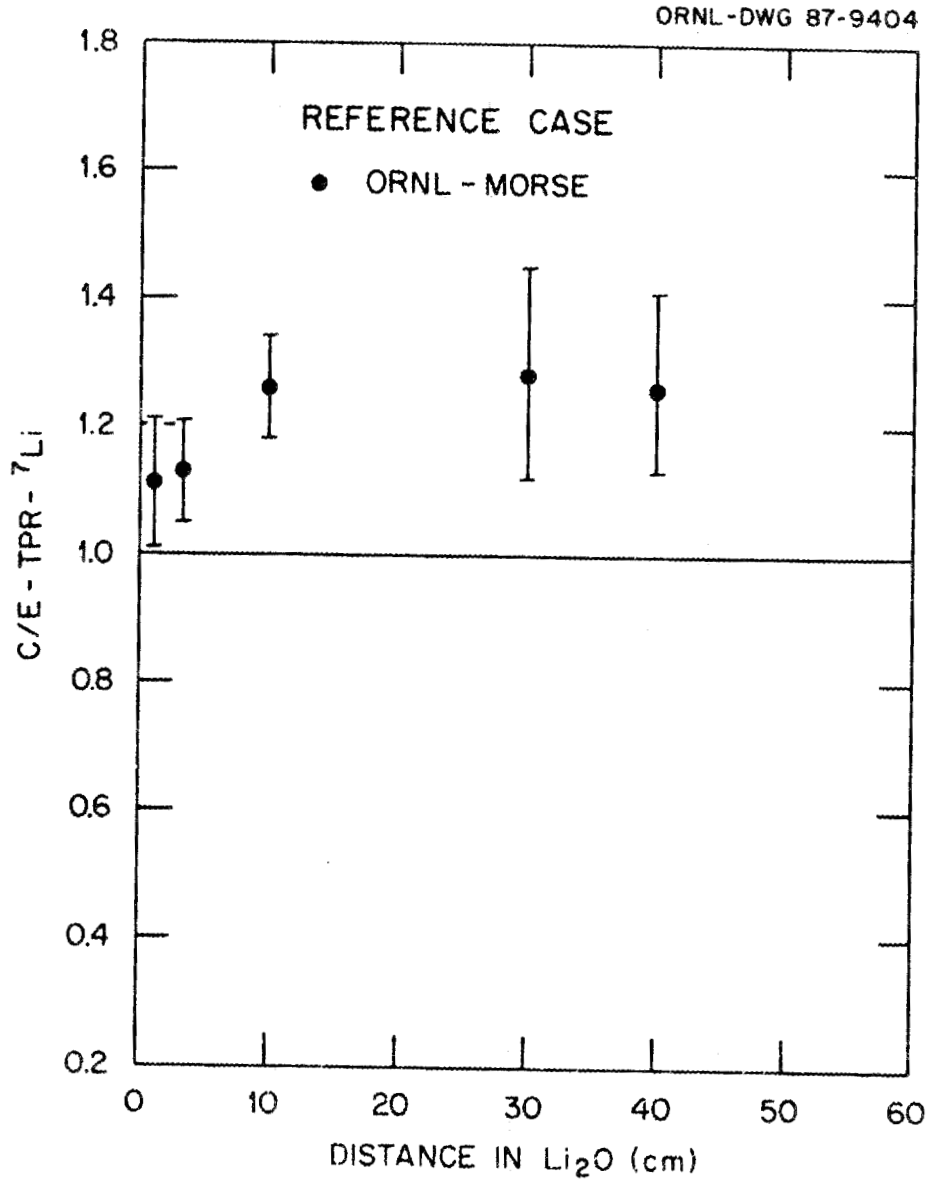

Figure 18. Calculated-to-Experimental Ratio for ^{7}Li Tritium Production vs Distance in the Li_2O Assembly--Reference Case.

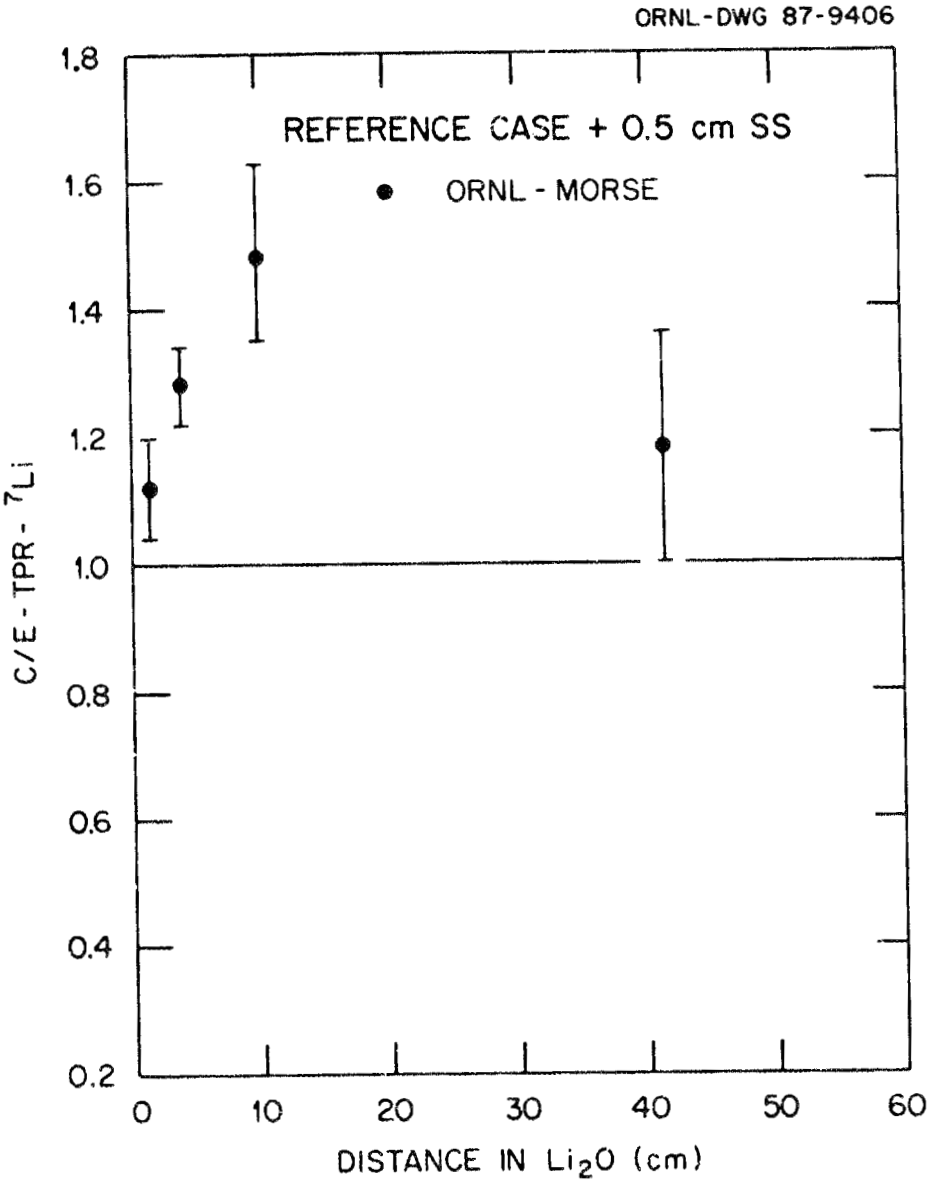

Figure 19. Calculated–to–Experimental Ratio for ^{7}Li Tritium Production vs Distance in the Li_2O Assembly with 0.5 cm–thick SS–304.

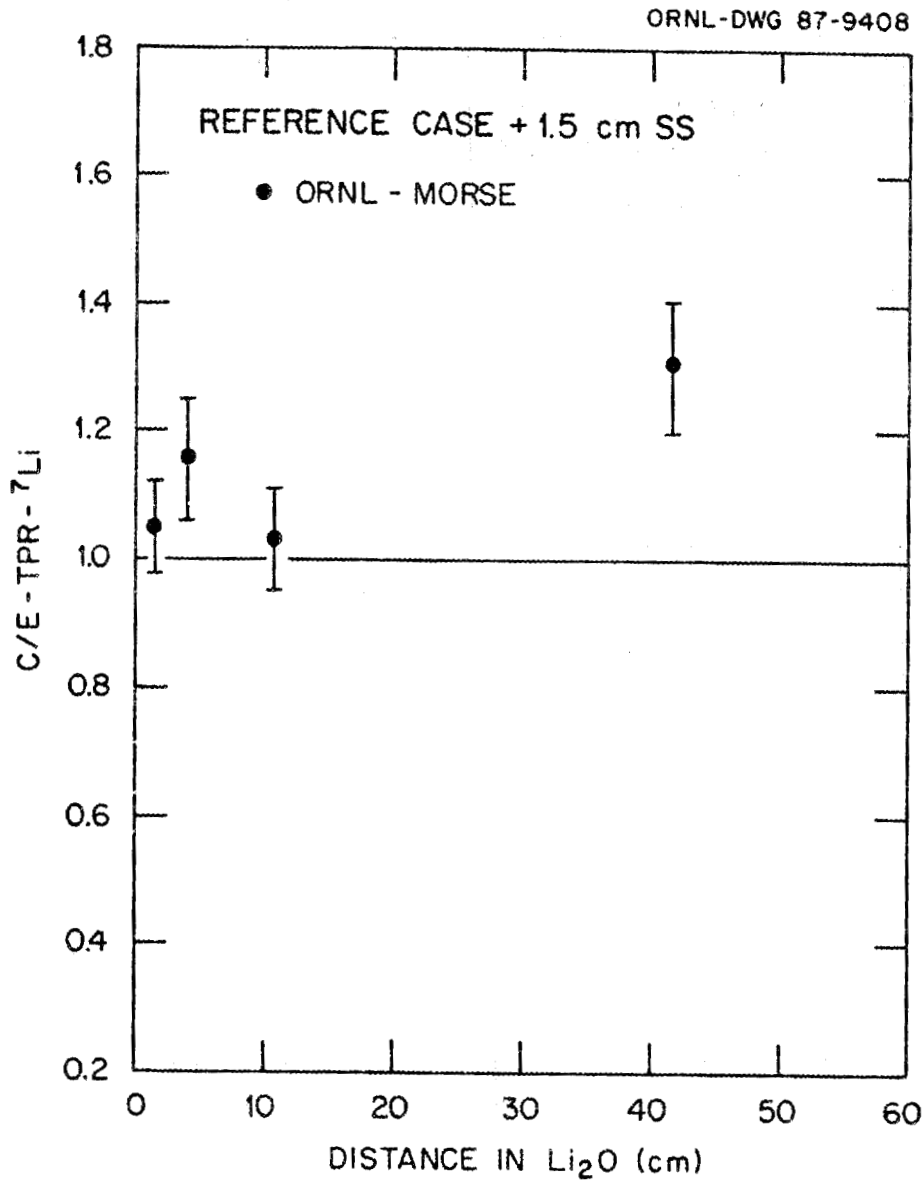

Figure 20. Calculated-to-Experimental Ratio for ^{7}Li Tritium Production vs Distance in the Li_2O Assembly with 1.5 cm-thick SS-304.

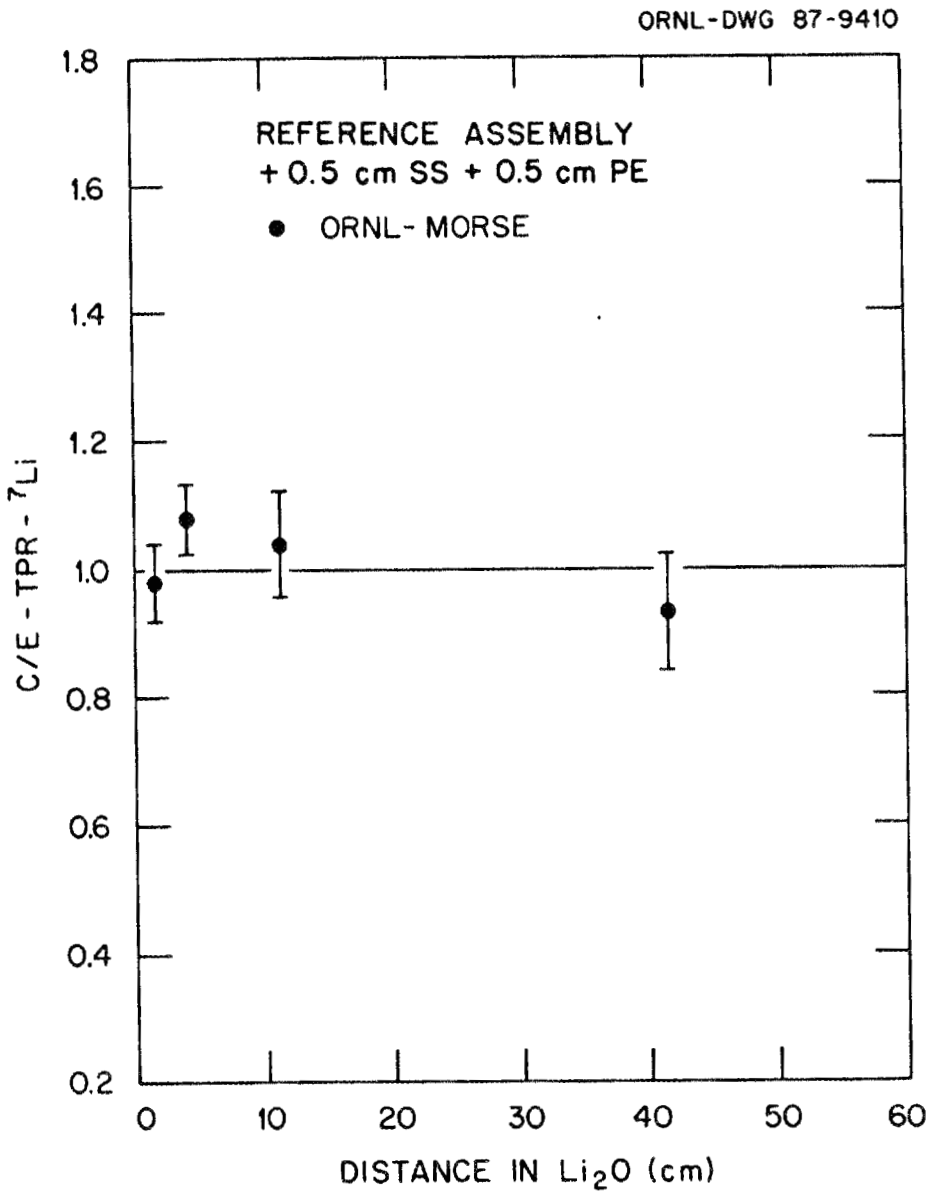

Figure 21. Calculated–to–Experimental Ratio for ^{7}Li Tritium Production vs Distance in the Li_2O Assembly with 0.5 cm–thick SS–304 and 0.5 cm–thick Polyethylene.

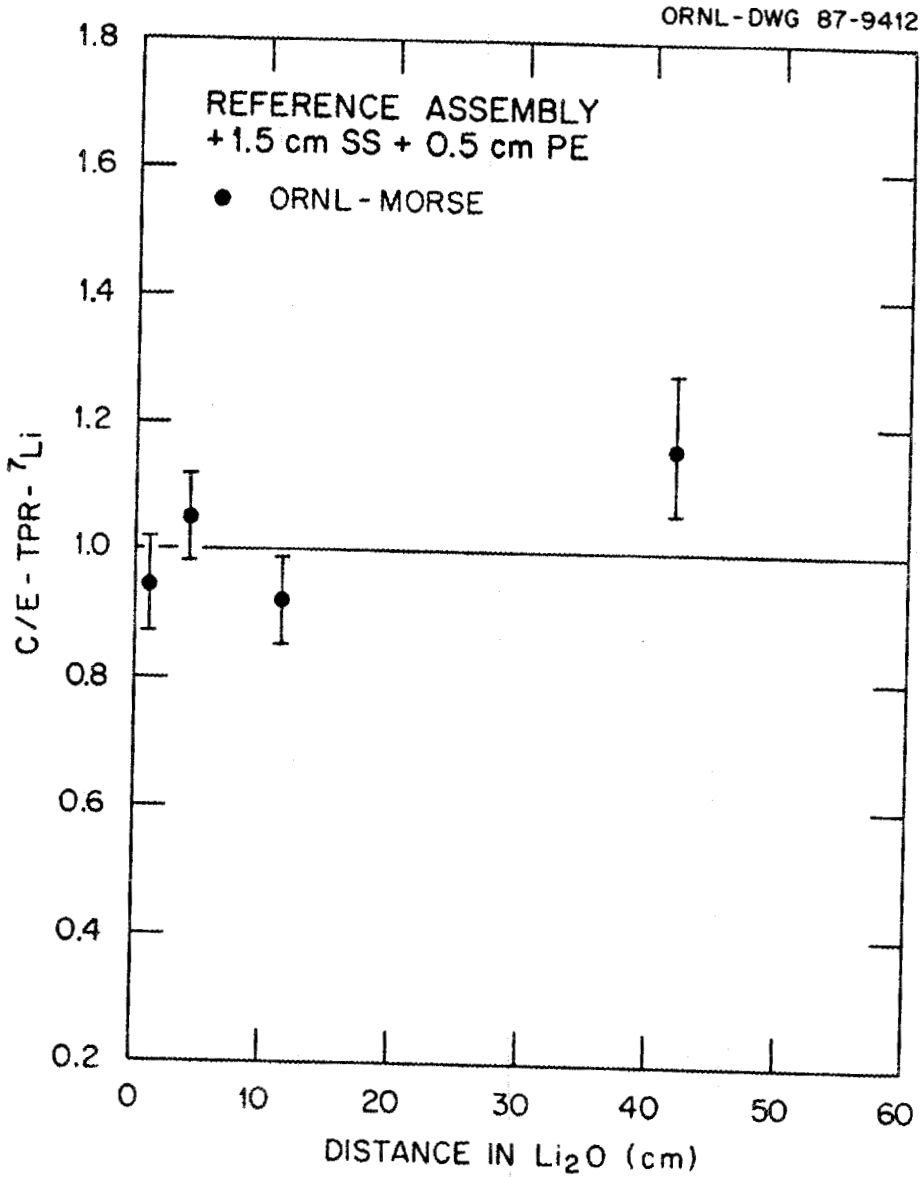

Figure 22. Calculated–to–Experimental Ratio for ^{7}Li Tritium Production vs Distance in the Li_2O Assembly with 1.5 cm–thick SS–304 and 0.5 cm–thick Polyethylene.

REFERENCES

1. U.S./JAERI Fusion Neutronics Calculational Benchmarks for Nuclear Data and Code Intercomparison, from the U.S./JAERI Collaborative Program on Fusion Neutronics (JR-1), PPG-900 UCLA-ENG-85-37 and JAERI-M 85-201 (December 1985), M. Z. Youssef, Editor.
2. The U.S./JAERI Second Workshop on Fusion Breeder Neutronics, June 19-21, 1986, Reno, Nevada, PPG-1000, UCLA-EGN-86-36 (August 1986), prepared by Mahmoud Z. Youssef.
3. M. B. Emmett, "The MORSE Monte Carlo Radiation Transport System," ORNL-4744, Oak Ridge National Laboratory (1975).
4. "MCNP — A General Purpose Monte Carlo Code for Neutron and Photon Transport," LA-7396-M (Rev. Version 2B) Los Alamos Monte Carlo Group, Los Alamos National Laboratory (1981).
5. T. Nakamura and M. A. Abdou, "Summary of Recent Results from the JAERI/U.S. Fusion Neutronics Phase I Experiments," *Trans. Amer. Nuc. Soc.* **52**, 1986 Annual Meeting, Reno, Nevada, June 15-19, 1986, p. 106.
6. H. Maekawa, T. Nakamura, M. Oyama, Y. Ikeda, S. Yamaguchi, K. Tsuda, K. Oishi (JAERI-Japan), K. G. Porges, E. F. Bennett, T. J. Yule, and D. J. D. Iorio (Argonne National Laboratory), "Measured Neutron Parameters for Phase I Experiments at the FNS," *Trans. Amer. Nuc. Soc.* **52**, 1986 Annual Meeting, Reno, Nevada, June 15-19, 1986, p. 109.
7. H. Maekawa, K. Tsuda, T. Iguchi, Y. Ikeda, Y. Oyama, T. Fukamoto, Y. Seki, and T. Nakamura, "Measurements of the Tritium Production Rate Distribution in Simulated Blanket Assemblies at the FNS," Japan Atomic Energy Research Institute, JAERI-M-83-196, 1983.
8. H. Maekawa, Y. Ikeda, Y. Oyama, S. Yamaguchi, K. Tsuda, T. Fukamoto, S. Kosako, M. Yoshizawi, and T. Nakamura, "Fusion Blanket Benchmark Experiments on a 60 cm-thick Lithium Oxide Cylindrical Assembly," Japan Atomic Energy Research Institute, JAERI-M-86-182, 1986.
9. R. T. Santoro, J. M. Barnes, J. D. Drischler, and R. G. Alsmiller, Jr., "Multigroup Energy-Angle Distributions for Neutrons from the $T(d,n)^4$He Reaction ($E_d = 100 - 400$keV)," Oak Ridge National Laboratory, ORNL/TM-9251.
10. C. R. Weisbin, R. W. Roussin, J. J. Wagschal, J. E. White, and R. Q. Wright, "VITAMIN-E: An ENDF/B-V Multigroup Cross-Section Library to LMFBR Core and Shield, LWR Shield, Dosimetry, and Fusion Blanket Technology," ORNL-5505, Oak Ridge National Laboratory (1979).
11. W. W. Engle, Jr., "A User's Manual for ANISN, A One-Dimensional Discrete Ordinates Transport Code with Anisotropic Scattering," K-1693, Oak Ridge National Laboratory (1967).
12. M. Z. Youssef, et al., "Analysis and Intercomparison for Phase I Fusion Integral Experiments at the FNS Facility," *Fusion Technology* **10**, 549-563 (1986).

INTERNAL DISTRIBUTION

1. F. S. Alsmiller
2–6. R. G. Alsmiller, Jr.
7. B. R. Appleton
8–12. J. M. Barnes
13. L. A. Berry
14–18. T. A. Gabriel
19. D. L. Henderson
20. D. T. Ingersoll
21. R. A. Lillie
22. F. C. Maienschein
23. R. W. Peelle
24. V. Protopopescu
25. R. W. Roussin
26. M. W. Rosenthal
27–31. R. T. Santoro
32. T. E. Shannon
33. C. R. Weisbin
34. EPMD Reports Office
35–36. Laboratory Records Department
37. Laboratory Records, ORNL-RC
38. Document Reference Section
39. Central Research Library
40. ORNL Patent Section

EXTERNAL DISTRIBUTION

41. S. E. Berk, Division of Development and Technology, Office of Fusion Energy, ER-532, U.S. Department of Energy, Washington, D.C. 20545
42. J. J. Dorning, Department of Nuclear Engineering and Engineering Physics, Thornton Hall, University of Virginia, Charlottesville, Virginia 22901
43. Y. Gohar, Argonne National Laboratory, 9700 S. Cass Avenue, Argonne, Illinois 60439
44. R. M. Haralick, Department of Electrical Engineering, University of Washington, Seattle, Washington 98195
45. Dr. Yasushi Seki, Japan Atomic Energy Research Institute, Tokai-mura, Ibaraki-ken, Japan
46. Thermonuclear Library, Japan Atomic Energy Research Institute, Tokai, Naka, Ibaraki, Japan
47. Office of the Assistant Manager for Energy Research and Development, Department of Energy, Oak Ridge Operations, P.O. Box 2001, Oak Ridge, TN 37831

48–57. Office of Scientific and Technical Information, P.O. Box 62, Oak Ridge, Tennessee 37830